

Nitrogen isotope and productivity variations along the northeast Pacific margin over the last 120 kyr: Surface and subsurface paleoceanography

Stephanie S. Kienast, Stephen E. Calvert, and Thomas F. Pedersen

Earth and Ocean Sciences, University of British Columbia, Vancouver, British Columbia, Canada

Received 26 April 2001; revised 5 March 2002; accepted 7 June 2002; published 15 October 2002.

[1] Glacial-interglacial changes in sedimentary $\delta^{15}\text{N}$ over the last 120 kyr display a remarkably similar pattern in timing and amplitude in core records extending from the denitrification zone in the eastern tropical North Pacific (ETNP), where subsurface denitrification is active, to the Oregon margin, where no denitrification occurs today. Low $\delta^{15}\text{N}$ values (4–6‰) generally characterize glacial stages 2 and 4, and higher $\delta^{15}\text{N}$ values (7–10‰) are representative of the Holocene, millennial-scale periods within stage 3, and stage 5. The inferred synchronicity of $\delta^{15}\text{N}$ variations along the entire margin implies that the nitrate isotopic signal produced in the oxygen-poor subsurface waters in the ETNP is rapidly advected northward and recorded at sites far beyond the boundaries of the modern denitrification zone. Similar to $\delta^{15}\text{N}$, primary production indicators (percent C_{org} , Ba/Al, and percent opal) show glacial-interglacial as well as millennial-scale variations along the NE Pacific margin, with higher primary production during warm periods. However, the relative phasing between $\delta^{15}\text{N}$ and paleoproduction tracers within individual records changes latitudinally. Whereas $\delta^{15}\text{N}$ and primary production vary approximately synchronously in the midlatitudes, production lags $\delta^{15}\text{N}$ in the ETNP by several kiloyears. This lag calls for a new understanding of the processes driving denitrification in the ETNP. We suggest that oxygen input by the Equatorial Undercurrent as well as local organic matter flux controls denitrification rates in the ETNP. Moreover, the differences in relative timing point to a time-transgressive development of upwelling-favorable winds along the NE Pacific margin after the last glaciation, with those in the north developing several kiloyears earlier. *INDEX TERMS:* 4267 Oceanography: General: Paleoceanography; 4870 Oceanography: Biological and Chemical: Stable isotopes; 4805 Oceanography: Biological and Chemical: Biogeochemical cycles (1615); 4845 Oceanography: Biological and Chemical: Nutrients and nutrient cycling; *KEYWORDS:* nitrogen isotopes, denitrification, California Current, California Undercurrent, paleoproduction

Citation: Kienast, S. S., S. E. Calvert, and T. F. Pedersen, Nitrogen isotope and productivity variations along the northeast Pacific margin over the last 120 kyr: Surface and subsurface paleoceanography, *Paleoceanography*, 17(4), 1055, doi:10.1029/2001PA000650, 2002.

1. Introduction

[2] The global carbon cycle is tightly coupled to that of nitrogen, and one of the current explanations for lower atmospheric CO_2 levels during the last glacial maximum (LGM) involves a stronger biological pump fueled by an increase in the store of oceanic nitrate [McElroy, 1983; Altabet et al., 1995, 1999a, 2002; Ganeshram et al., 1995, 2000; Falkowski, 1997]. Biologically available, fixed nitrogen is the main limiting nutrient in most of today's ocean [Dugdale and Goering, 1967; Codispoti, 1989], and changes in its oceanic reservoir size, which mainly consists of nitrate (NO_3^-), may therefore play a key role in regulating Earth's climate via the uptake of CO_2 during photosynthetic primary production.

[3] The major sources of fixed nitrogen to the ocean are terrestrial run off and marine nitrogen fixation. The main sink is sedimentary denitrification in shallow continental shelf sediments and water column denitrification in the

eastern tropical North Pacific (ETNP), the eastern tropical South Pacific (ETSP), and the Arabian Sea (AS). In the oxygen-poor subsurface waters ($[\text{O}_2] < 10 \mu\text{mol}$) of these areas, bacteria use nitrate as an electron acceptor to degrade organic matter and produce N_2 and the greenhouse gas N_2O , both of which are lost to the atmosphere [Cline and Kaplan, 1975; Codispoti and Christensen, 1985; Law and Owens, 1990; Naqvi et al., 1998, 2000]. Isotopically lighter $^{14}\text{NO}_3^-$ is preferred over the heavier $^{15}\text{NO}_3^-$ during denitrification with a substantial fractionation factor ($\epsilon = 25\text{--}30\%$; [Cline and Kaplan, 1975; Brandes et al., 1998; Voss et al., 2001]). Denitrification therefore leads to the accumulation of isotopically highly enriched nitrate, as evidenced by $\delta^{15}\text{N}_{\text{nitrate}}$ values of up to 18‰ in the ETNP (Figure 1) at subsurface depths [Cline and Kaplan, 1975]. Biological nitrogen fixation, on the other hand, the conversion of the abundant, but inert N_2 gas to NH_4^+ by some marine cyanobacteria, adds new fixed nitrogen to the ocean. Almost no isotope fractionation occurs during N_2 fixation [Wada and Hattori, 1976], and newly fixed nitrate has an isotopic composition close to that of the atmospheric N_2 substrate, which is, by definition, 0‰. Sediments can be faithful

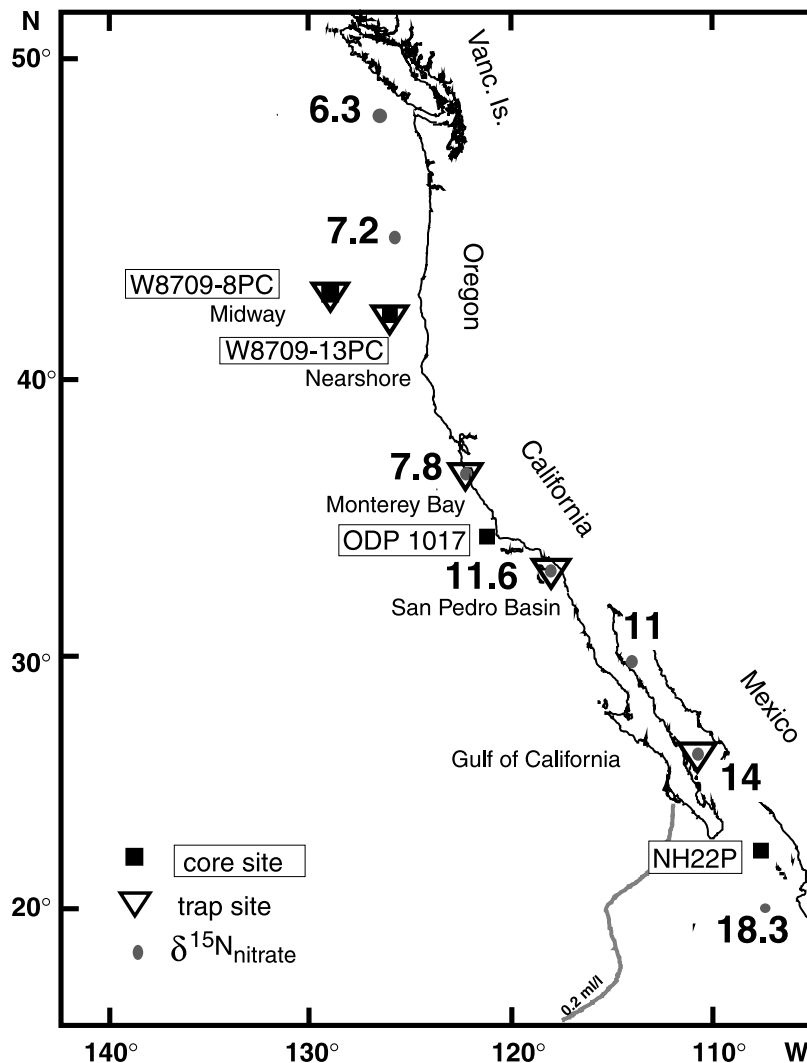


Figure 1. Map of the midlatitude NE Pacific margin with Multitracers core (solid squares) and sediment trap (inverse triangles) sites Nearshore and Midway. Other core sites mentioned in the text are ODP Hole 1017E off California and NH22P off Mexico [Ganeshram *et al.*, 1995, 2000]. Other sediment trap sites include Monterey Bay, San Pedro Basin, and Carmen Basin in the Gulf of California [Altabet *et al.*, 1999b]. Numbers (solid circles) indicate maximal water column $\delta^{15}\text{N}_{\text{nitrate}}$ values between 100 and 350 m taken from Cline and Kaplan [1975] (ETNP); Pride *et al.* [1999] (Gulf of California); Altabet *et al.* [1999b] (San Pedro Basin and Monterey Bay). Stippled line (0.2 mL/L O_2 at 400 m depth, from NOAA) indicates approximate boundary of the denitrification zone.

recorders of the isotopic composition of oceanic nitrate when nitrate uptake by primary producers in the euphotic zone is complete and there is no diagenetic alteration of the isotopic signal as it sinks and is buried in sediments as particulate nitrogen (PN).

[4] Observational support for glacial-interglacial changes in the marine nitrogen budget comes from sedimentary records from the Arabian Sea and the eastern tropical North and South Pacific [Altabet *et al.*, 1995, 1999a, 2002; Ganeshram *et al.*, 1995, 2000]. Glacial sediments in these regions are characterized by lower $\delta^{15}\text{N}$ ($\sim 5\text{--}6\text{‰}$) compared with higher values ($\sim 8\text{--}9\text{‰}$) during the Holocene. This pattern has been interpreted to reflect reduced denitrification, and, by inference, an increased nitrate reservoir

in the glacial ocean, an interpretation that has been challenged by sedimentary nitrogen isotope records from the South China Sea [Kienast, 2000]. Under conditions of complete nitrate utilization, changes in $\delta^{15}\text{N}$ of particulate nitrogen in the euphotic zone overlying an active denitrification area can potentially be affected by a) changes in the rate of denitrification at subsurface depths due to a variable supply of oxygen or of degradable organic matter, and b) changes in the strength of vertical transport of isotopically heavy NO_3^- to the surface. Outside of denitrification zones, $\delta^{15}\text{N}$ of particulate nitrogen can additionally be influenced by changes in horizontal advection of nitrate with a preformed isotopic signature. Distinguishing between these different processes has not previously been attempted.

Table 1. Multitracer Sediment Traps and Sediment Cores Used in This Study

	Longitude, °W	Latitude, °N	Depth, m
	<i>Nearshore</i>		
Traps	125°45.00'	42°05.00'	
Cores			
W8709A-13PC	125°45.00'	42°07.01'	2712
W8709A-9BC	125°49.28'	42°04.72'	2824
	<i>Midway</i>		
Traps	127°35.00'	42°10.00'	
Cores			
W8709A-8TC	127°40.68'	42°15.74'	3111
W8709A-8PC	127°40.68'	42°15.74'	3111
W8709A-6BC	127°38.31'	42°15.24'	2914

[5] In this study we present new $\delta^{15}\text{N}$ and primary production records of sediment cores and sediment traps (Table 1) from the Multitracers Experiment off the Oregon margin [Lyle *et al.*, 1992]. No local water column denitrification occurs in this region today; nevertheless, the sediment cores show a very similar glacial-interglacial $\delta^{15}\text{N}$ pattern to those from the ETNP and the AS. These $\delta^{15}\text{N}$ results are evaluated in light of the sediment trap results, regional $\delta^{15}\text{N}_{\text{nitrate}}$ data, and hydrographic conditions. Paleo-export production is reconstructed using the sedimentary concentrations of biogenic opal and organic carbon (C_{org}) as well as Ba/Al ratios. The phase relationships between $\delta^{15}\text{N}$ and primary production proxies in the Multitracers cores are then compared to the phasing in core records from within (off northwestern Mexico) and outside (off California) the denitrification zone in the ETNP. This comparison offers new insight into the effects of vertical and horizontal circulation changes on the $\delta^{15}\text{N}$ signal in marine sediments along the NW American margin. A full understanding of these processes may lead to the use of $\delta^{15}\text{N}$ as a water mass tracer for the present [Brandes *et al.*, 1998] and the past ocean.

2. Hydrography of the Study Area

[6] The coastal region of the NE Pacific lies under the influence of the California Current System (CCS), which represents the eastern boundary current of the clockwise rotating current gyre in the North Pacific. The CCS includes the broad (1000 km) but shallow (0–300 m) southward flowing California Current (CC) at the surface and the narrow (10–40 km) poleward flowing California Undercurrent (CUC) at greater depths. The CC transports cooler, low salinity and highly oxygenated water from the Subarctic equatorward [Hickey, 1998] whereas the CUC carries warmer, salty, and oxygen-depleted water of equatorial origin to the north [Wooster and Jones, 1970; Hickey, 1979, 1998; Gardner, 1982; Pierce *et al.*, 2000]. Recently, it was pointed out that the CUC also exports a substantial amount of nitrogen from the ETNP to the north [Castro *et al.*, 2001].

[7] The CCS is associated with intense coastal upwelling driven by northerly, alongshore winds that are generated by the pressure gradient between the North Pacific High pressure cell and a thermal low over California. The winds result in offshore Ekman transport of surface water and large-scale vertical movement of nutrient-rich subsurface

water to the sea surface, supporting high primary production along the entire northwestern American coast [Hickey, 1998]. Onshore return flow of water to compensate offshore Ekman transport off Oregon occurs roughly from depths between 100 and 200 m [Huyer, 1983; Van Geen *et al.*, 2000]. This is within the depth range of strongest CUC flow (100–300 m) [Wooster and Jones, 1970; Hickey, 1979, 1998; Gardner, 1982; Pierce *et al.*, 2000].

[8] At the southern end of the CCS (south of $\sim 25^\circ\text{N}$), relatively old and oxygen-poor subsurface and intermediate waters impinge on the continental margin. In combination with the high downward flux of organic matter derived from primary production, this causes a thick oxygen minimum zone (OMZ) between 150–800 m depth. In the upper part of the OMZ, roughly between 100 and 500 m, dissolved oxygen concentrations drop below $5 \mu\text{M}$, and bacterial water column denitrification becomes the dominant respiratory process [Cline and Kaplan, 1975; Brandes *et al.*, 1998; Voss *et al.*, 2001]. Subsurface $\delta^{15}\text{N}_{\text{nitrate}}$ values are thus markedly enriched off northwestern Mexico and in the southern Gulf of California, but decrease progressively to the north (Figure 1).

3. Productivity Proxies

[9] We reconstruct past primary production using three independent proxies, percent opal, percent organic carbon and the barium/aluminum ratio.

3.1. Opal

[10] Cold, recently upwelled waters in the CCS region support a high biomass of various diatom species [Hood *et al.*, 1990, 1991; Chavez *et al.*, 1991], and diatoms overwhelmingly dominate the microfossil assemblage found in all Multitracers trap samples [Sancetta, 1992]. Although the presence of opal-rich sediments is clearly associated with high primary productivity in coastal upwelling areas [e.g., Calvert and Price, 1983], the relationship between silica production and opal accumulation is not straightforward as seawater is undersaturated with respect to silicic acid [Archer, 1993; Ragueneau *et al.*, 2000]. Consequently, opal dissolves during settling through the water column and at the sediment surface. The physical and biological conditions of upwelling areas such as the CCS region, however, promote opal burial through pulsed upwelling events that support extensive blooms of large, heavily silicified and chain-forming diatoms species with a tendency to form aggregates, as well as through grazing by zooplankton and subsequent fecal pellet production [Nelson *et al.*, 1995; Ragueneau *et al.*, 2000]. All of these factors effectively shorten the exposure time of opal particles to seawater by increasing their settling rate. Down core enrichments in sedimentary opal are therefore used here as a qualitative indicator of past periods of relatively high diatom production.

3.2. Organic Carbon

[11] Along with biogenic opal, organic carbon is a direct product of marine primary production and its flux below the euphotic zone is a function of net primary production at the surface and depth-dependent degradation [Suess, 1980]. Numerous studies in a variety of oceanic settings have

demonstrated an overall positive relationship between primary production, organic carbon export and organic carbon burial [Müller, 1979; Sarnthein, 1988; Calvert *et al.*, 1992, 1995; Pedersen *et al.*, 1992]. However, the exact conditions under which organic carbon supplied to the sediments is preserved are still subject to debate. High sedimentation rates [e.g., Müller, 1979] as well as physical protection of organic matter by the inorganic matrix of sinking particles [Hedges *et al.*, 2001] have been suggested to enhance organic carbon preservation, whereas exposure to oxygen [Hartnett *et al.*, 1998] has been proposed to reduce it. Recently, the rate at which fresh organic matter is degraded in the water column has been shown to be the same in anoxic basins and the open ocean [Thunell *et al.*, 2000], indicating that exposure to oxygen is not the overriding control on the preservation of organic matter. In addition, the importance of surface productivity in controlling not only the sedimentary organic carbon content but also the local bottom water oxygen content was highlighted by Stott *et al.* [2000] in a recent study in the borderland basins of the NE Pacific. These authors showed that the superposition of bioturbated sediments (requiring bottom water oxygen) upon laminated sediments (deposited under anoxic or near anoxic bottom water) was caused by an overall reduction in coastal upwelling, i.e. marine production, over the course of the 20th century.

[12] Comparing the C_{org} rain rate in the 1000 m sediment trap to the C_{org} accumulation rate at the seafloor at the Multitracer sites, Lyle *et al.* [1992] found that more than 20% of the entire C_{org} flux through the water column is preserved in the sediment. Moreover, sedimentation rate changes since the LGM seem to have been too small to have affected C_{org} preservation [Lyle *et al.*, 1992]. In LGM sediments, the total organic matter content is reduced and the terrestrial organic carbon fraction is about twice as large as during the Holocene [Lyle *et al.*, 1992]. Subtracting the terrestrial C_{org} input from the total organic carbon content will therefore only amplify the pattern of lower C_{org} values during glacials.

3.3. Barium

[13] In addition to organic carbon and biogenic opal, barium (Ba) was quantified in the Midway core as a paleoproduction proxy. Barite (BaSO_4) has been shown to be precipitated in microenvironments containing decaying organic matter and the remains of siliceous plankton [Bishop, 1988]. A large set of sediment trap data has led to the definition of quantitative algorithms relating new production in the euphotic zone to biogenic barium accumulation rates in sediments [Dymond *et al.*, 1992; Franois *et al.*, 1995; Dymond and Collier, 1996]. Pore waters at hemipelagic sites such as the Midway site are usually saturated with respect to barite [Church and Wolgemuth, 1972] and barite is well preserved. Since the Midway site is also free of major detrital Ba contamination, it is well suited for Ba-based paleoproduction estimates. Rather than estimating biogenic barium as $[\text{bioBa}] = ([\text{Ba}] - 0.0075 [\text{Al}])$ [Dymond *et al.*, 1992], we directly report the ratio of total barium to aluminum (Ba/Al).

[14] Although both opal and organic carbon suffer from degradation and dissolution effects, the factors considered

responsible for their preservation (e.g. opal solution vs. organic matter flux and/or oxygen exposure) are different. The combined use of these two proxies and their comparison with barium, a more refractory chemical species, should therefore help to reliably hindcast paleoproduction changes in a semi-quantitative manner.

4. Materials and Methods

[15] The Multitracers Experiment on the Oregon margin combined measurements of water column tracer fluxes with studies of down core variations in sediment burial fluxes [Lyle, 1992]. Trap moorings were deployed 120 km ("Near-shore") and 270 km ("Midway") off the coast from September 1987 to September 1991. Box and piston cores at these sites (Table 1) were collected on board the R/V *Wecoma* in 1987. The traps collected particle flux at 1000, 1500, 1750, and 2300 m depth in cups that were changed automatically at bimonthly to biweekly time intervals (or after 6–12 months for bulk samples). Details of the trap design are given by Dymond and Lyle [1994]. Nitrogen isotope ratios of the trap samples were determined using a Fisons NA1500 elemental analyzer coupled to a VG prism mass spectrometer in a continuous flow of helium. Analytical precision is $\pm 0.2\text{‰}$ (1σ) and the values are reported relative to air N_2 . Subsamples of the Multitracers cores were freeze-dried and manually homogenized in an agate mortar. Total carbon was determined by flash-combustion gas chromatography with a Carlo Erba NA1500 elemental analyzer using operational conditions similar to those described by Verardo *et al.* [1990]. Sulfanilamide and several certified rock standards were used to calibrate the instrument. Relative standard deviation (R.S.D.) was $\pm 2\%$ (1σ) based on several standards analyzed along with the samples. Inorganic carbon was determined directly by CO_2 evolution after HCl treatment of the sediment sample in a carbon dioxide coulometer with an analytical precision of $\pm 2.3\%$ (1σ , R.S.D.). Organic carbon was estimated by subtracting inorganic from total carbon, with a combined analytical precision (as R.S.D.) of $\pm 3\%$. Biogenic opal was determined by alkaline extraction of silica [Mortlock and Froelich, 1989] from 20 mg sub-samples into a 2 M Na_2CO_3 solution at 85°C for 5 hours. Percent opal is calculated as 2.4% Si_{opal} . The precision based on a sediment standard containing 11.6% opal analyzed along with the samples was $\pm 4.3\%$ (1σ). Barium (Ba) and aluminum (Al) were determined using a Philips 2400 wavelength-dispersive sequential automatic X-ray fluorescence spectrometer. Dry powdered sediment was fused at 1100°C and cast into a glass disk for Al analyses, and pressed into a borax-backed pellet for Ba analyses. Precision for both elements was better than $\pm 4\%$ (1σ , R.S.D.). Details of sample preparation, instrumental conditions and correction methods are given by Calvert *et al.* [1985]. Sedimentary nitrogen isotope ratios were determined using the same methods as for the sediment trap samples.

[16] Water column samples for nitrate isotopic analyses were collected at 150 and 600 m off Oregon ($125^\circ 05.78' \text{W}$, $44^\circ 40.126' \text{N}$, July 1999, $n = 4$) and at 200 and 400 m depth off Vancouver Island ($126^\circ 40.03' \text{W}$, $48^\circ 38.91' \text{N}$, August 2001, $n = 2$). Isotopic analyses were carried out

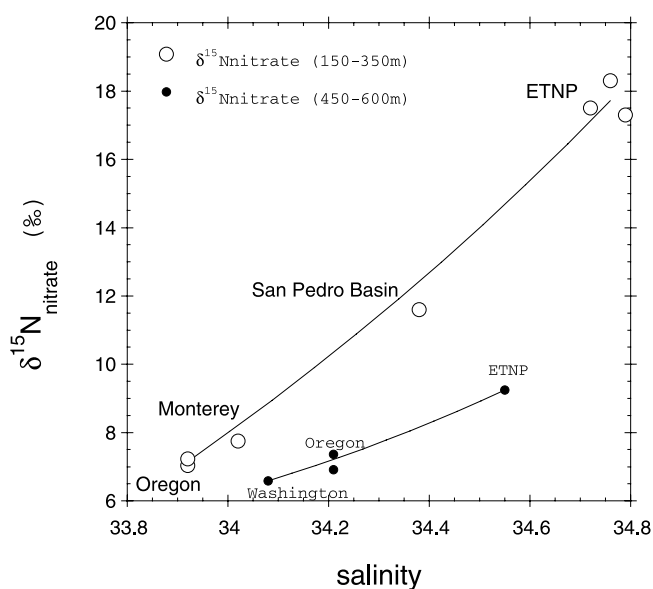


Figure 2. Relationship between $\delta^{15}\text{N}_{\text{nitrate}}$ and salinity of samples from the California Current region. Open circles indicate samples originating from 150–350 m water depth; solid circles indicate deeper samples. The solid lines are ideal mixing lines following Liu and Kaplan [1989]. This mixing relationship illustrates that waters from the ETNP are an important source of isotopically heavy nitrate to the entire NW American margin. See Figure 1 caption for $\delta^{15}\text{N}_{\text{nitrate}}$ references; salinity data are from Liu and Kaplan [1989] (ETNP and San Pedro Basin), F. Chavez and R. Michisaki (unpublished data, 2002) (Monterey Bay); M. Lyle (unpublished data, 1987) (Oregon), and Brandes [1996] (Washington).

after extraction of nitrate from seawater followed by diffusion onto acidified glass fiber filters [Sigman *et al.*, 1997]. Data were kindly provided by M. Altabet (Oregon samples) and J. Needoba and M. Kienast (Vancouver Island samples). Other $\delta^{15}\text{N}$ nitrate data shown in Figures 1 and 2 are compiled from the literature. The heaviest values between 100–350 m from Monterey Bay, San Pedro and the ETNP, where full water column profiles of $\delta^{15}\text{N}_{\text{nitrate}}$ are available, are shown in Figure 1 and in Figure 2 (open circles).

5. Chronostratigraphy

[17] The age model for Nearshore core W8709-13PC is presented in detail by Mix *et al.* [1999] and Lund and Mix [1998]. From 0–36 kyr (0–557 cm), it is based on 41 AMS ^{14}C dates on planktonic and benthic foraminifera [Mix *et al.*, 1999]. From 36–59 kyr (557–760 cm) the age model is based on correlating millennial-scale oxygen isotope peaks to North Atlantic core V23-81 as well the identification of the marine oxygen isotope stage 3–4 boundary at 59 kyr [Lund and Mix, 1998]. The chronology of the remaining core length (760–858.5 cm) was approximated for this study by linearly extrapolating the sedimentation rate.

[18] Piston core Midway (W8709A-8 PC) was spliced with its trigger core W8709A-8 TC based on a comparison

of magnetic susceptibility and CaCO_3 records in both cores, which indicated that the piston core overpenetrated by 140 cm [Lyle *et al.*, 1992]. A new chronostratigraphy of this composite record was established for this study based on a correlation (not shown) of its high resolution CaCO_3 content to a radiocarbon and oxygen-isotope dated, stacked carbonate record from the California margin [Lyle *et al.*, 2000]. Kiloyear-scale CaCO_3 and C_{org} events are a common feature in this area and can be used with care for chronostratigraphic control [Karlin *et al.*, 1992; Lyle *et al.*, 2000]. The resulting age model corresponds to the previously used radiocarbon based chronology of W8709-8 PC [Lyle *et al.*, 1992; Doose *et al.*, 1997] for the last 30 kyr, but is more accurate in the older part of the record, where the previous model was based on the assumption of linear sedimentation rates only.

[19] The age model of Mexican margin core NH22P is described in detail by Ganeshram and Pedersen [1998], and the age model of ODP Hole 1017E will be published elsewhere (Hendy and Pedersen, manuscript in preparation, 2002).

[20] The absolute accuracy of the individual age models is not crucial in the context of this study. Our conclusions are based on the phase relationship between (1) different proxies within the same core and (2) the same proxy relative to the benthic $\delta^{18}\text{O}$ signal in different cores. The glacial-interglacial $\delta^{18}\text{O}_{\text{benthic}}$ transition is assumed to be recorded simultaneously at comparable depths along the NW American margin.

6. Results

6.1. Water Column and Sediment Trap Results off Oregon

[21] The $\delta^{15}\text{N}_{\text{nitrate}}$ at the Multitracer sites at 150 and 600 m is 7.1‰ on average ($n = 4$, Figure 3) whereas values of 6.1 and 6.3‰ occur off Vancouver Island at 200 and 400 m depth, respectively. For comparison, the global ocean average is estimated to be around 4.5–5‰ [Sigman *et al.*, 1997], and deep water values of 4–5‰ are observed in the NE Pacific [Cline and Kaplan, 1975; Wu *et al.*, 1997]. $\delta^{15}\text{N}$ of settling particulate nitrogen ($\delta^{15}\text{N}_{\text{PN}}$) collected in cups that were open for 6–12 months varies from 7.9 to 5.9‰ at the Nearshore site and from 8.8 to 5.4‰ at the Midway site with averages of 7.0 and 7.4‰, respectively (Figure 3). These averages are similar to the isotopic composition of the surface sediment at both sites (6.5‰ and 8.0‰ at Nearshore and Midway, respectively). The composite isotopic time series from September 1987 to September 1991 shows a distinct seasonal cycle of $\delta^{15}\text{N}_{\text{PN}}$ depletion (4–6‰) and enrichment (8‰), with lighter values generally occurring in spring and fall and heavy values occurring in summer. Maxima in opal flux (not shown (R. Dymond, unpublished data, 1998)) occur shortly after $\delta^{15}\text{N}_{\text{PN}}$ minima. Superimposed on the seasonal $\delta^{15}\text{N}$ pattern is an overall increase in $\delta^{15}\text{N}$ from 1987 to 1991.

6.2. Sediment Core Results

[22] The Multitracers cores show a clear glacial-interglacial pattern in export production over the last 120 ka, with low organic carbon, opal and barium contents during cold

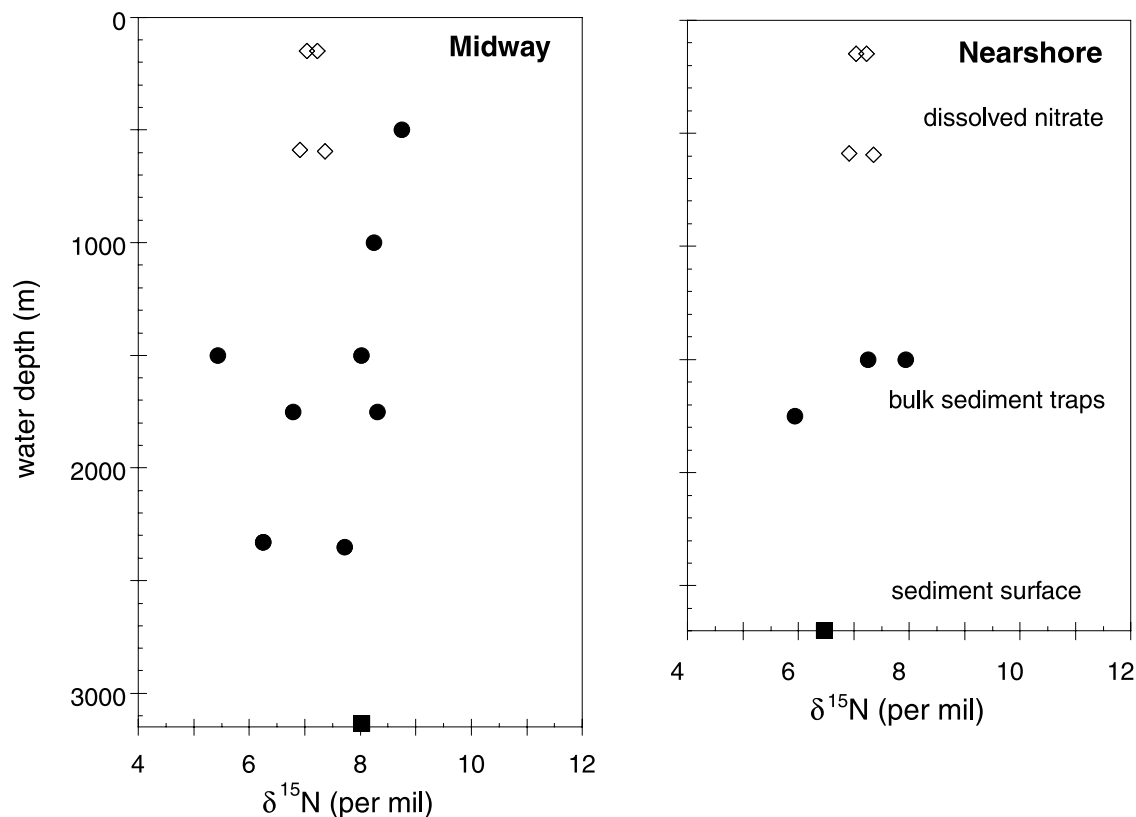


Figure 3. Nitrogen isotopic composition of dissolved nitrate off Oregon (diamonds, samples taken in July 1999 at $125^{\circ}05.78'W$, $44^{\circ}40.126'N$) compared with bulk sediment trap samples representing 6–12 months (circles) and box core surfaces (squares) at the Nearshore and Midway sites.

oxygen isotope stages 2 and 4 and values almost twice as high during the Holocene and stage 5 (Figures 4 and 5). Stage 3 also shows several millennial-scale paleoproduction proxy fluctuations with amplitudes approximately half as large as the glacial-interglacial contrast. In the higher resolution core W8709-13PC, organic carbon and opal percentages decrease to an intermittent minimum around 11 ka B.P. after an initial increase during the last termination. The increase to maximum Holocene values in organic carbon concentrations is quite abrupt, whereas opal and Ba/Al increase more gradually and reach maximum Holocene values slightly after $\%C_{org}$. The three different paleoproduction proxies consistently show reduced primary production during stages 2 and 4 compared to the Holocene and stage 5.

[23] Sedimentary $\delta^{15}\text{N}$ values are low during the glacial (4–6‰), higher during the interglacials (7–10‰) and show millennial scale fluctuations during oxygen isotope stage 3 (Figures 4 and 5). Apart from a $\delta^{15}\text{N}$ maximum around 19 kyr B.P., organic carbon and $\delta^{15}\text{N}$ covary closely in Nearshore core W9709-13PC and the transitions from oxygen isotope stages 4 to 3 and from 2 to 1 as well as most fluctuations of both proxies during stage 3 occur approximately synchronously (Figure 4). This is true for Midway core W8709-8PC as well, although from stage 5 to stage 2 the coupling between barium and $\delta^{15}\text{N}$ is tighter than that between C_{org} and $\delta^{15}\text{N}$ (Figure 5). The relationship between

opal and $\delta^{15}\text{N}$ is somewhat weaker. Thus, although maybe not strictly coupled, $\delta^{15}\text{N}$ covaries approximately in phase with paleoproduction proxies off Oregon.

7. Interpretation

7.1. Water Column and Sediment Trap Data

[24] Subsurface $\delta^{15}\text{N}_{nitrate}$ measurements from the NE Pacific are still sparse, but the available data from the NW American margin show that they progressively decrease from high values in the ETNP (18.3‰) to lower values farther north (7.2‰ off Oregon; Figure 1). Despite this decrease, they are still higher than the global ocean average of 4.5–5‰ [Sigman *et al.*, 1997] and deep water values of 4–5‰ observed in the NE Pacific [Cline and Kaplan, 1975; Wu *et al.*, 1997]. Using $\delta^{15}\text{N}_{nitrate}$ and salinity data, Liu and Kaplan [1989] suggested that the subsurface $\delta^{15}\text{N}_{nitrate}$ maximum observed in the San Pedro Basin off southern California is imported from the ETNP by the CUC. Based on the data compiled in Figures 1 and 2, we argue that this transport continues to the Oregon coast, possibly even farther north to Vancouver Island. In Figure 2, $\delta^{15}\text{N}_{nitrate}$ in the CCS is plotted versus salinity. The ideal mixing lines for two depth ranges are constructed following the approach outlined by Liu and Kaplan [1989] and using data from the ETNP and from Oregon (for samples from 150–350m depth), and from the ETNP and Washington (for samples

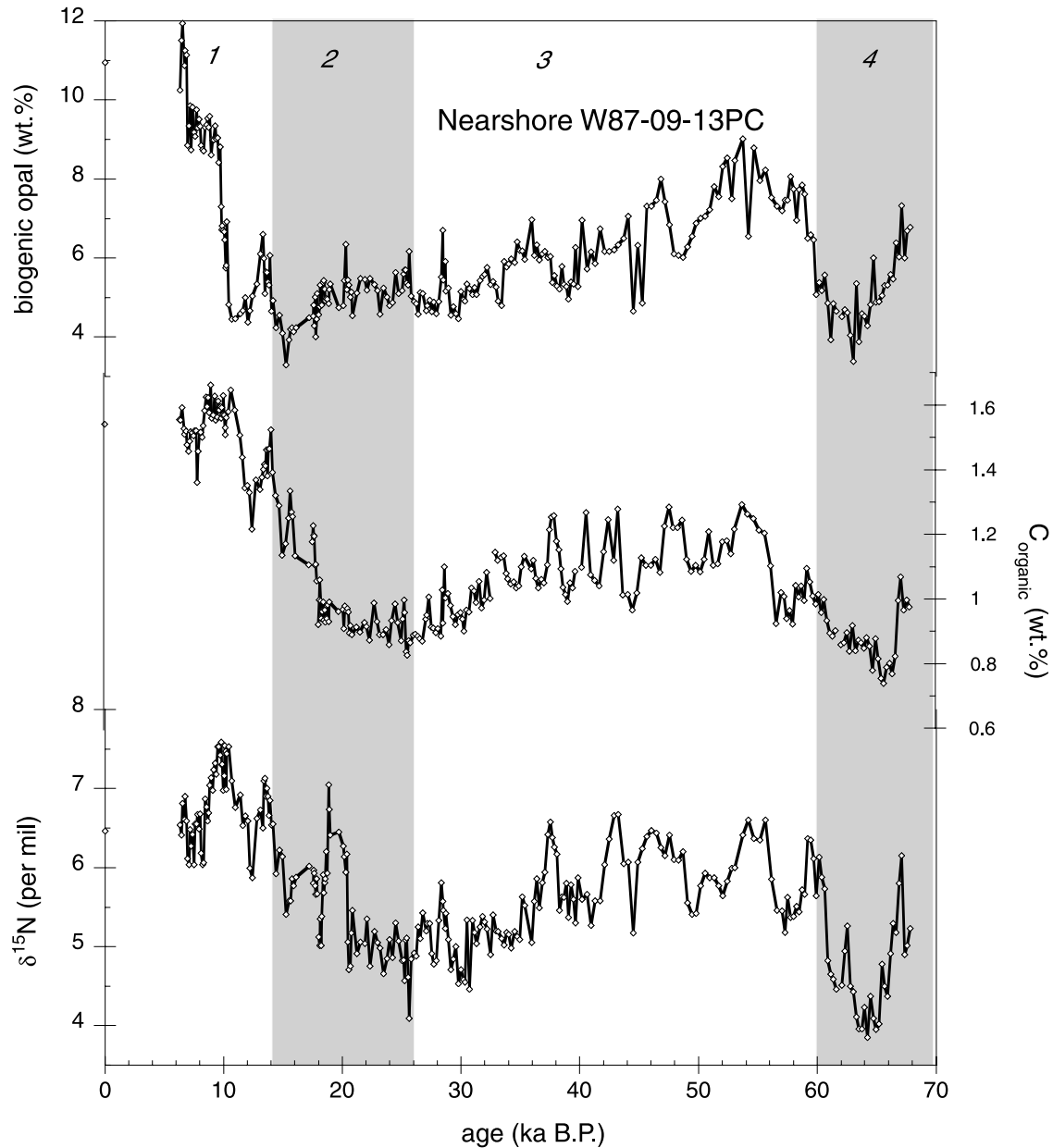


Figure 4. Sedimentary $\delta^{15}\text{N}$, organic carbon, and biogenic opal concentrations versus age from Nearshore core W8709-13PC off Oregon. Timescale is from *Mix et al.* [1999] and *Lund and Mix* [1998]. Diamonds on y axes indicate surface sediment values from corresponding box core. Italic numbers indicate marine oxygen isotope stages.

from 450–600 m depth) as end-members. Most of the data fall on or near the ideal mixing lines, indicating that waters derived from the ETNP are indeed an important source of isotopically heavy nitrate for the northern CCS region. The CUC is most likely the main transport mechanism since it flows poleward from the ETNP to Vancouver Island along this coastline [*Pierce et al.*, 2000; *Castro et al.*, 2001]. In addition, heavy nitrate might also homogeneously spread northward as well as westward via lateral mixing from the ETNP. There are not enough $\delta^{15}\text{N}_{\text{nitrate}}$ data available yet to test this, however.

[25] Additional support for the influence of the CUC comes from the three-year sediment trap time series off Oregon (Figure 6). It shows a clear seasonal cycle in $\delta^{15}\text{N}_{\text{PN}}$, with lighter values in spring and fall most likely reflecting changes in relative nutrient utilization, i.e. the balance between physical supply of nitrate by upwelling and its consumption by phytoplankton uptake over the course of one year [*Wada and Hattori*, 1978; *Altabet and Franois*, 1994]. The relationship between opal flux maxima (not shown), indicating upwelling, and isotopic minima corroborates this assertion [*Altabet*, 1996]. However, there is also

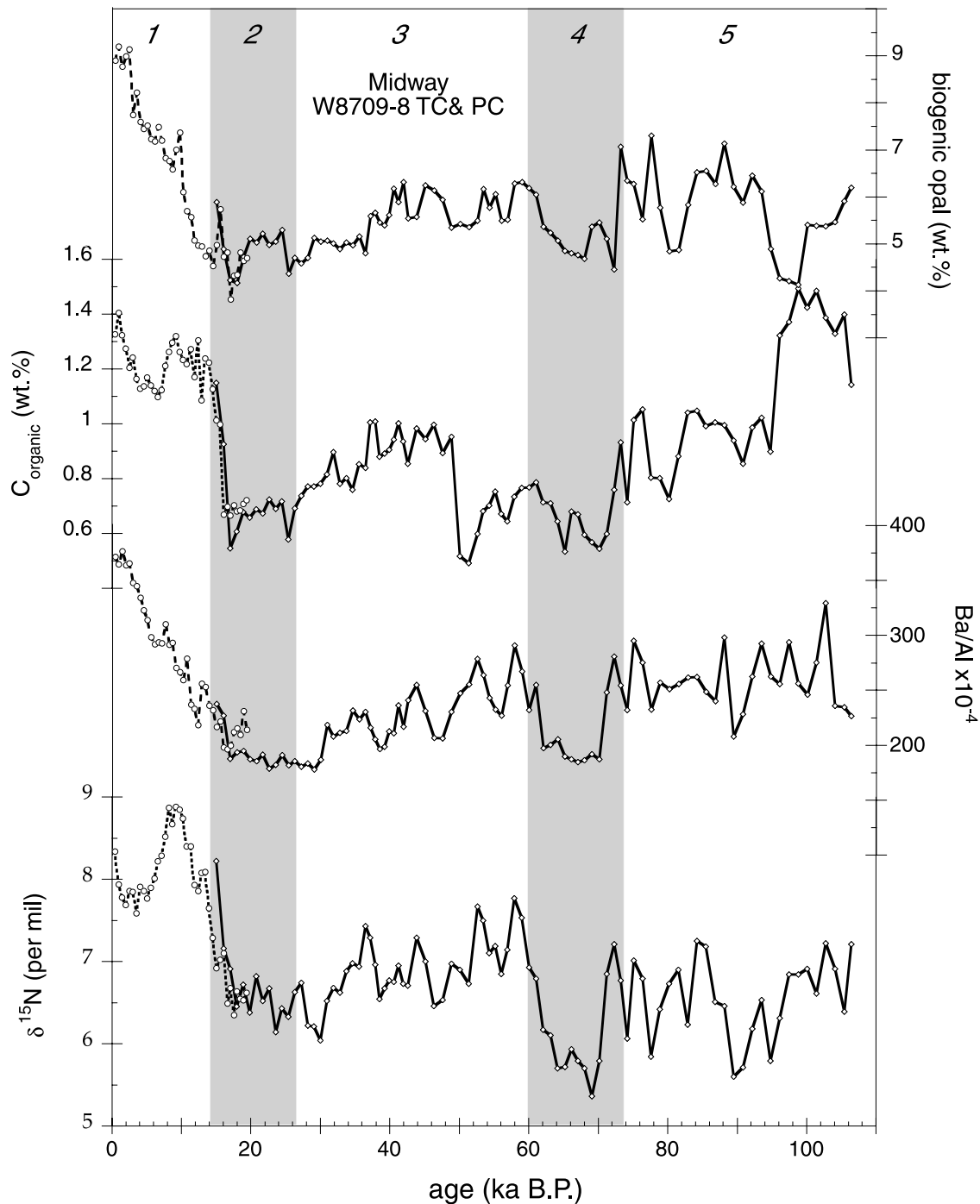


Figure 5. Sedimentary $\delta^{15}\text{N}$, Ba/Al ratios, organic carbon, and biogenic opal concentrations of Midway cores W8709-8PC and W8709-8TC off Oregon versus age. Timescale is described in text. Italic numbers indicate marine oxygen isotope stages.

an overall trend toward higher $\delta^{15}\text{N}_{\text{PN}}$ values from 1987 to 1991, which is superimposed on the seasonal $\delta^{15}\text{N}_{\text{PN}}$ pattern. Sediment traps from Monterey Bay, ca. 400 km farther south, also show heavier $\delta^{15}\text{N}_{\text{PN}}$ values from late 1991 to early 1992 compared with the two previous years [Altabet *et al.*, 1999b]. The end of the Multitracers time series coincides with the beginning of the 1991–1992 El Niño period.

During El Niño events, CUC flow is unusually strong [Hickey, 1998], and increased undercurrent flow has been directly observed off Oregon at the onset of the 1982–1983 El Niño [Huyer and Smith, 1985]. The increased import of heavy nitrate caused by a stronger CUC may therefore explain the trend toward higher $\delta^{15}\text{N}_{\text{PN}}$ observed in sediment trap time series off Oregon and Monterey Bay.

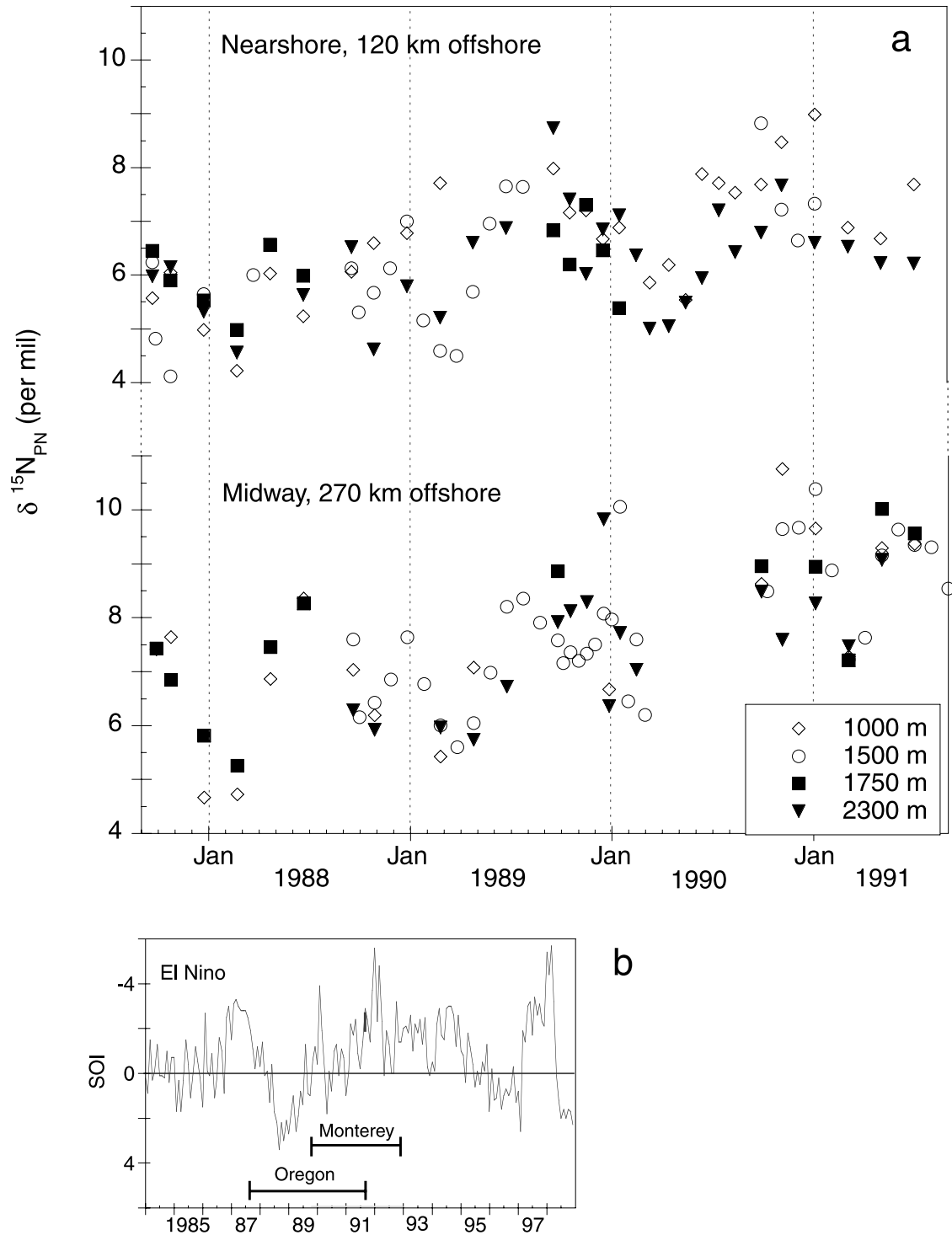


Figure 6. (a) Multitracers $\delta^{15}\text{N}_{\text{PN}}$ trap time series off Oregon from September 1987 to September 1991. Note the lack of a systematic change with depth and the increasing trend toward the end of the time series. (b) Multitracers and the Monterey Bay sediment trap deployment periods (horizontal bars) relative to the Southern Oscillation Index (SOI). Negative SOI values indicate El Niño conditions.

[26] Although there is some year-to-year $\delta^{15}\text{N}_{\text{PN}}$ variation in the bulk sediment trap samples (Figure 3), the sediment surface $\delta^{15}\text{N}$ values (6.5 and 8.0‰ at Nearshore and Midway, respectively) fall well within the range of the trap samples

and are very close to their average composition (7.0 and 7.4‰ at Nearshore and Midway, respectively). This indicates that there is no significant diagenetic offset at the sediment water interface. We note, however, that the more offshore

Midway site does have a 1.5‰ heavier core top $\delta^{15}\text{N}$ despite no large difference in %C_{org} (Figure 5). The average composition of settling PN is in turn very similar to that of dissolved nitrate (7.1‰) off Oregon (Figure 3). Surface nitrate concentrations over the annual cycle at the Nearshore and Midway sites are low (1–2 $\mu\text{mol/L}$ [Levitus *et al.*, 1994]). If all upwelled nitrate is taken up by primary producers and converted to PN, and if sinking PN is the only significant loss term, then mass balance dictates that the isotopic composition of the product equals that of the substrate [Altabet and McCarthy, 1985; Altabet, 1988]. These conditions of complete nitrate utilization over the course of one year seem to apply at the Multitracers sites. Complete nitrate utilization and the absence of diagenetic alteration of the isotopic signal has also been inferred at Monterey Bay, San Pedro Bay, and Carmen Basin farther south in the CC region [Altabet *et al.*, 1999b; Pride *et al.*, 1999], and they most likely represent regional phenomena along the North American coast. This means that the seasonal differences in relative nitrate utilization seen in the time series will not be recorded in the sediment. Rather, the $\delta^{15}\text{N}$ composition of the Multitracers cores is a recorder of the mean $\delta^{15}\text{N}$ of subsurface nitrate imported from the ETNP by the CUC.

7.2. Down Core Records

7.2.1. Primary Production

[27] The sedimentary concentrations of opal, organic carbon and the Ba/Al ratio consistently show reduced primary production during stages 2 and 4 compared to the Holocene, stage 3 and stage 5. Reduced coastal upwelling and primary production during the LGM have previously been inferred off Oregon [Lyle *et al.*, 1992; Sancetta *et al.*, 1992; Ortiz *et al.*, 1997], California [Dean *et al.*, 1997; Gardner *et al.*, 1997] and Mexico [Ganeshram and Pedersen, 1998]. Building on model simulations [COHMAP, 1988], Lyle *et al.* [1992] and Ganeshram and Pedersen [1998] argue that the semi-permanent high pressure cell over the Laurentide ice cap caused a weaker and more southerly North Pacific high pressure cell during the LGM, which can explain the widespread reduction of upwelling favorable winds along the entire Northwest American margin.

[28] The deglacial rise in %C_{org} is interrupted by three intermittent C_{org} minima in the higher resolution core W8709-13PC (Figure 4). The third and most pronounced minimum occurs between 13.6 and 11.6 ka B.P., supporting findings by Mix *et al.* [1999] and Pisias *et al.* [2001] that coastal upwelling off Oregon and northern California was significantly lower during a period possibly correlative to the Younger Dryas event. During stage 3, periods of relatively intense production every 5–10 kyr are interrupted by four periods of reduced upwelling. In a model of the response of the Pacific North West to the North Atlantic Heinrich events [Hostetler and Bartlein, 1999] lowering the Laurentide ice sheet during ice surges induces changes in upper level and surface winds over western North America, which in turn significantly reduce northerly, upwelling-favorable summer winds over Oregon and northern California. Similarly, Pisias *et al.* [2001] infer that at wavelengths >3000 years, warm events in Greenland are correlated to intervals of increased coastal upwelling off

Oregon. A direct correlation of the millennial-scale upwelling events recorded in the Multitracers cores to events elsewhere is difficult because of the errors associated with marine sedimentary chronologies, but in light of the results by Hostetler and Bartlein [1999] and Pisias *et al.* [2001] we suggest that the periods of reduced upwelling might correspond to Heinrich events and that the periods of stronger upwelling might correspond to the most pronounced Dansgaard-Oeschger interstadials as recorded in GISP2.

[29] Primary production during stage 5 was higher than during the cold stages 2 and 4. However, the signals are quite variable and, for example, an increase in %opal between 100 and 94 ka B.P. coincides with a decrease in %C_{org} in W8709-8PC (Figure 5). This is similar to findings from nearby ODP site 1020 during this time and probably reflects the individual signature of MIS 5 compared to the Holocene [Lyle *et al.*, 2001].

7.2.2. $\delta^{15}\text{N}$

[30] In principle, the glacial-interglacial $\delta^{15}\text{N}$ variations observed in the Multitracers cores could reflect differences in nutrient utilization and/or denitrification. However, given that nitrate uptake is complete under modern conditions of intense coastal upwelling, and assuming that there were no major changes in phytoplankton assemblages, nitrate uptake most likely was complete during the LGM, when upwelling was reduced [Lyle *et al.*, 1992; Sancetta *et al.*, 1992; Ganeshram and Pedersen, 1998]. Therefore changes in relative nitrate utilization over time can be discounted as an explanation for the observed sedimentary $\delta^{15}\text{N}$ variations. Local denitrification during the Holocene, stage 3 and stage 5 is unlikely, as the lowest dissolved O₂ concentrations in subsurface waters off Oregon today (~18 μM , between 500–1000 m [Levitus *et al.*, 1994]) are not low enough to support local denitrification. During the glacial stages, lower organic matter flux through the water column would have diminished oxygen consumption, possibly leading to even higher dissolved O₂ concentrations.

[31] The Multitracers sediment traps and surface sediment data together with the isotopic composition of modern subsurface nitrate strongly suggest that the $\delta^{15}\text{N}$ composition of the Multitracers cores record the $\delta^{15}\text{N}$ of subsurface nitrate, which today is characterized by an isotopically heavy signature imported from the ETNP by the CUC. Higher sedimentary $\delta^{15}\text{N}$ values during the Holocene, parts of stage 3 and during stage 5 therefore imply that the CUC and the processes that drive it have most likely been in existence during these times. Simultaneously, paleoproduction proxies indicate that northerly winds drove coastal upwelling during at least a portion of the year. Thus, during the Holocene, parts of stage 3 and stage 5, these components of the CCS seem to have been working in a similar fashion as today.

[32] In contrast, the lower $\delta^{15}\text{N}$ values during glacial stages 2 and 4 can be interpreted in several ways. First, the glacial reduction in coastal upwelling [Lyle *et al.*, 1992; Sancetta *et al.*, 1992; Ganeshram and Pedersen, 1998] would have caused less upwelling of isotopically heavy nitrate into the euphotic zone. A deepening of the thermocline would have had the same effect (see discussion below). Secondly, as denitrification in the ETNP was

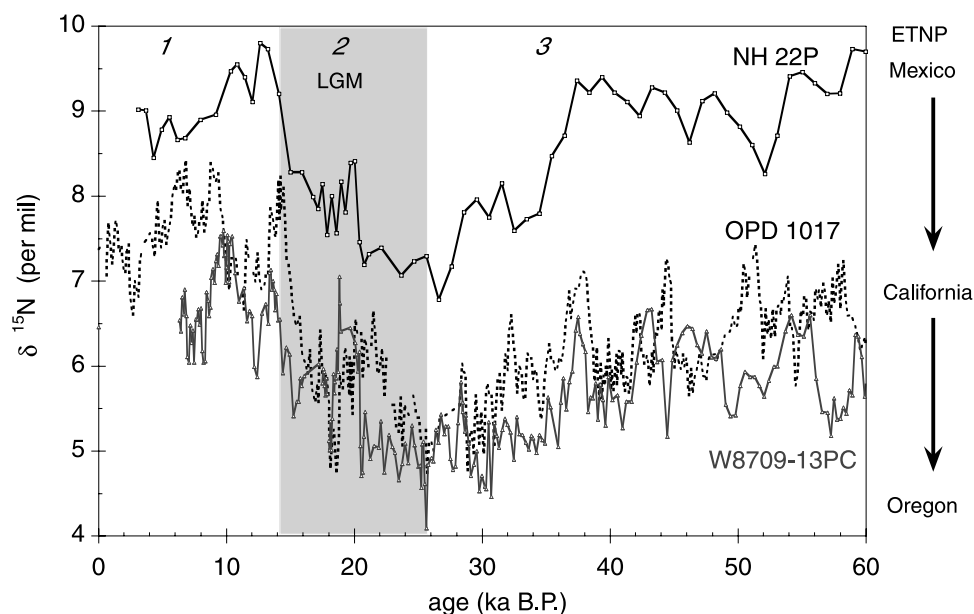


Figure 7. Sedimentary $\delta^{15}\text{N}$ records from the Mexican (NH22P), Californian (ODP 1017E), and Oregon (W8709-13PC) margins over the last 60 kyr plotted according to their independent age models. The $\delta^{15}\text{N}$ record of ODP Hole 893A [Emmer and Thunell, 2000] from the Santa Barbara Basin (not shown) is similar to that of Hole 1017E.

weakened [Ganeshram *et al.*, 1995, 2000], the isotopic signal exported from the ETNP would have been lower than today and, by the time it reached Oregon, too diluted to be distinguishable from that of average oceanic nitrate. Thirdly, the CUC was most likely weaker, because of a weaker CC during the LGM [Doose *et al.*, 1997; Herbert *et al.*, 2001] and because the CUC is strongest today in the summer when the surface-flowing CC is strongest [Hickey, 1998]. A weaker CUC would have led to reduced importation of heavy nitrate to the Oregon site. We cannot currently distinguish between the above scenarios because the $\delta^{15}\text{N}$ minima in the Oregon cores (4–6‰) are similar to the isotopic composition of mean oceanic nitrate. Most likely, a combination of them (i.e. a reduction in production, horizontal and vertical advection of heavy nitrate) caused the CCS region to lose its distinctive isotopic signature during the glacials and instead to be indistinguishable from the mean oceanic nitrate pool. Information on the $\delta^{15}\text{N}_{\text{nitrate}}$ in the glacial ocean outside of denitrification zones is still quite limited, although it might not have been very different from today [Kienast, 2000]. Thus the Oregon margin was no longer connected to the denitrification zone via the CUC but belonged to a different regime. At the same time denitrification in the ETNP was reduced, leading to lower sedimentary $\delta^{15}\text{N}$ values off Mexico. Interestingly, the glacial-interglacial amplitude of 2–3‰ is the same in both regions. This, however, is most likely fortuitous.

8. Discussion

8.1. Comparison of the Oregon Sites With Other Records from the NE Pacific

[33] In spite of covering a distance of over 2000 km, the transect of $\delta^{15}\text{N}$ variations from Oregon and California to

Mexico displays a remarkably similar and most likely synchronous (see below) pattern over the last 60 kyr (Figure 7). Comparable to the spatial trend in modern $\delta^{15}\text{N}_{\text{nitrate}}$ values, sedimentary $\delta^{15}\text{N}$ decreases with distance from the ETNP. The record from ODP Hole 1017E off California can also be explained by variations in the advection of isotopically heavy nitrate from the ETNP, similar to the Oregon cores (see section 7.2 and Emmer and Thunell [2000]). During the Holocene and during stage 3, $\delta^{15}\text{N}$ values in core 1017E are 0.5–1‰ higher than in core W8709-13PC off Oregon, whereas both cores show the same minimal values between 26–30 kyr B.P. Changes in $\delta^{15}\text{N}$ and paleoproduction proxies in the Oregon cores are closely in phase on a sample to sample basis, and the same is true for $\delta^{15}\text{N}$ and C_{org} in ODP Hole 1017E off California [see Ganeshram *et al.*, 2000, Figure 3] and also for $\delta^{15}\text{N}$ and biogenic opal in core JPC-56 from the central Gulf of California [Pride *et al.*, 1999]. While paleoproduction tracers therefore appear to respond more or less in phase with sedimentary $\delta^{15}\text{N}$ outside the ETNP, the two proxies are out of phase within the denitrifying zone off the Mexican margin. In this area, the rise in C_{org} during the last termination lags that of $\delta^{15}\text{N}$ by several kiloyears [Ganeshram *et al.*, 1995, Figure 1; Ganeshram *et al.*, 2000, Figure 3] and the same lag is observed at the stage 4/3 and 6/5 boundaries. In view of this considerable lag, variations in primary production in this region cannot have been the sole control on the intensity of denitrification in this area.

8.2. What Drives Glacial-Interglacial Variations in Sedimentary $\delta^{15}\text{N}$?

[34] Changes in the isotopic composition of PN in the euphotic zone overlying an active denitrification area such as the ETNP can be caused by two different processes. The

first is a change in the vertical transport of isotopically heavy nitrate to the surface where it is then assimilated by phytoplankton and incorporated into sedimenting particles. The second process is a variation in either the supply of oxygen or of organic matter, both of which induce a change in the intensity of denitrification. Both of these mechanisms, changing thermocline depth and changing denitrification intensity, can be tested as possible candidates for explaining the glacial-interglacial $\delta^{15}\text{N}$ variations in the NE Pacific.

8.2.1. Thermocline hypothesis

[35] Changes in the vertical upward flux of isotopically heavy nitrate can be achieved by deepening the thermocline and allowing less water from the subthermocline denitrification zone to be tapped and upwelled. Conversely, raising the thermocline would facilitate the vertical transport of isotopically heavy nitrate into the euphotic zone. Consistent with this hypothesis, *Altabet et al.* [1999b] observed that the $\delta^{15}\text{N}$ of new nitrogen delivered to the sea surface in the modern Gulf of California decreased during the 1991–92 El Niño event, when the main thermocline in the eastern tropical Pacific deepened [*Philander*, 1990]. However in areas such as the ETNP, where organic matter flux is important in maintaining low subsurface O_2 concentrations, this mechanism can only operate on short (interannual) timescales. On longer timescales, an increase in thermocline depth will also reduce the upward flux of subthermocline nutrients and consequently primary production will decrease. Such a deepening of the thermocline should therefore be recorded as a synchronous decrease in sedimentary $\delta^{15}\text{N}$ and primary production, which is not observed at the Mexican margin sites.

8.2.2. Equatorial and California Undercurrent hypothesis

[36] The depletion of O_2 and the potential for denitrification at a particular location depend on the amount of oxidizable material present and the supply of O_2 to this location by circulation and diffusion [*Wyrski*, 1962, 1967]. In the modern ETNP, the secondary nitrite maximum and the heavy $\delta^{15}\text{N}_{\text{nitrate}}$ peak, both of which are results of active denitrification, are observed between 100–500 m depth with maximal values at around 250 m [*Cline and Kaplan*, 1975; *Garfield et al.*, 1983] and 350–400 m [*Brandes et al.*, 1998], respectively. The water mass in this depth range is Subtropical Subsurface Water (SSW, after *Wyrski* [1967]). It is characterized by its high salinity (>34.6) and has the identical temperature, salinity, and density properties as the “13°C Water” described by *Tsuchiya* [1981]. 13°C Water acquires its initial properties in the western South Pacific and is transported to the ETNP by the Equatorial Undercurrent (EUC) [*Tsuchiya*, 1981; *Tsuchiya et al.*, 1989; *Toggweiler et al.*, 1991]. At the Galapagos Islands, most of the water from the EUC spreads south and north and continues to flow poleward along the eastern boundaries of the Pacific Ocean [*Tsuchiya*, 1981; *Lukas*, 1986]. The initially high oxygen content of EUC water is consumed rapidly under the highly productive surface waters in the eastern tropical Pacific [*Wyrski*, 1967]. As pointed out by *Ganeshram et al.* [2000], only circulation or ventilation changes in this subsurface water mass have the potential to affect denitrification rates in

the ETNP, not changes in the deeper part of the OMZ, which consist of North Pacific Intermediate Water.

[37] The EUC mostly owes its existence to the easterly trade winds. They force the oceanic upper layer to pile up at the western boundary of the Pacific basin and thereby establish a zonal horizontal pressure gradient toward the east. The trade winds form the lower limb of the thermally produced Hadley cell, which in the northern hemisphere is strongest in winter when the equator-pole temperature gradient is intensified. Cooling of the polar regions is thought to compress and intensify the Hadley cell [*Nicholson and Flohn*, 1980; *Flohn*, 1982] and paleoceanographic data indeed suggest stronger atmospheric circulation and trade winds during the LGM [e.g., *Molina-Cruz*, 1977; *Sarnthein et al.*, 1981; *Pedersen*, 1983; *Parkin and Shackleton*, 1973; *Paytan et al.*, 1996]. The model based results of *Bush and Philander* [1999] and *Andreasen et al.* [2001] suggest that stronger glacial easterlies increase the E-W tilt of the tropical thermocline in the central Pacific and double the speed of the EUC. The computed changes in thermocline depth agree with foraminiferal evidence collected from sediments deposited during the LGM [*Andreasen and Ravelo*, 1997]. An increase in EUC speed should increase O_2 advection into the ETNP and reduce denitrification during cold stages, independent of local productivity changes. As the injection of O_2 in this hypothesis is an atmosphere-driven mechanism, it would be able to decrease the intensity of denitrification in the ETNP in concert with the millennial-scale climate coolings such as the Dansgaard-Oeschger stadials and Heinrich events observed in the North Atlantic region. During warm stages, on the other hand, with little O_2 advection and intense denitrification in the ETNP, the CUC could easily propagate the heavy nitrate signal northward along the entire NW American margin within a few months. As OPD site 1017 is located closer to the source region, it shows slightly higher $\delta^{15}\text{N}$ values (by 0.5–1‰) than the core records off Oregon during these times (Figure 7). During cold periods and reduced denitrification in the ETNP, however, $\delta^{15}\text{N}$ values in the Oregon and the California cores are the same as both most likely recorded the isotopic composition of mean oceanic nitrate. The suggested scenario would result in a synchronous, continental-margin wide sedimentary $\delta^{15}\text{N}$ response reaching far beyond the boundaries of the ETNP that is in phase with the transition from glacial (stadial) to interglacial (interstadial) periods.

[38] In the southern hemisphere, the poleward Peru Undercurrent is the equivalent of the CUC and its connection with the EUC is well documented [*Tsuchiya*, 1981; *Lukas*, 1986; *Toggweiler et al.*, 1991]. The mechanism described above could therefore operate in the southern Hemisphere as well and thereby synchronize $\delta^{15}\text{N}$ records along the NE and SE Pacific margins. No data are yet in hand to support this suggestion, however.

[39] The glacial-interglacial $\delta^{18}\text{O}$ transition in benthic foraminifera should be recorded at the same time off Mexico and off Oregon. The timing of the $\delta^{18}\text{O}$ change in Mexican core NH 22P based on its radiocarbon chronology [*Ganeshram and Pedersen*, 1998] corresponds indeed to that in core 13PC off Oregon, independently dated using radiocarbon dates (Figure 8, top). This good correspondence

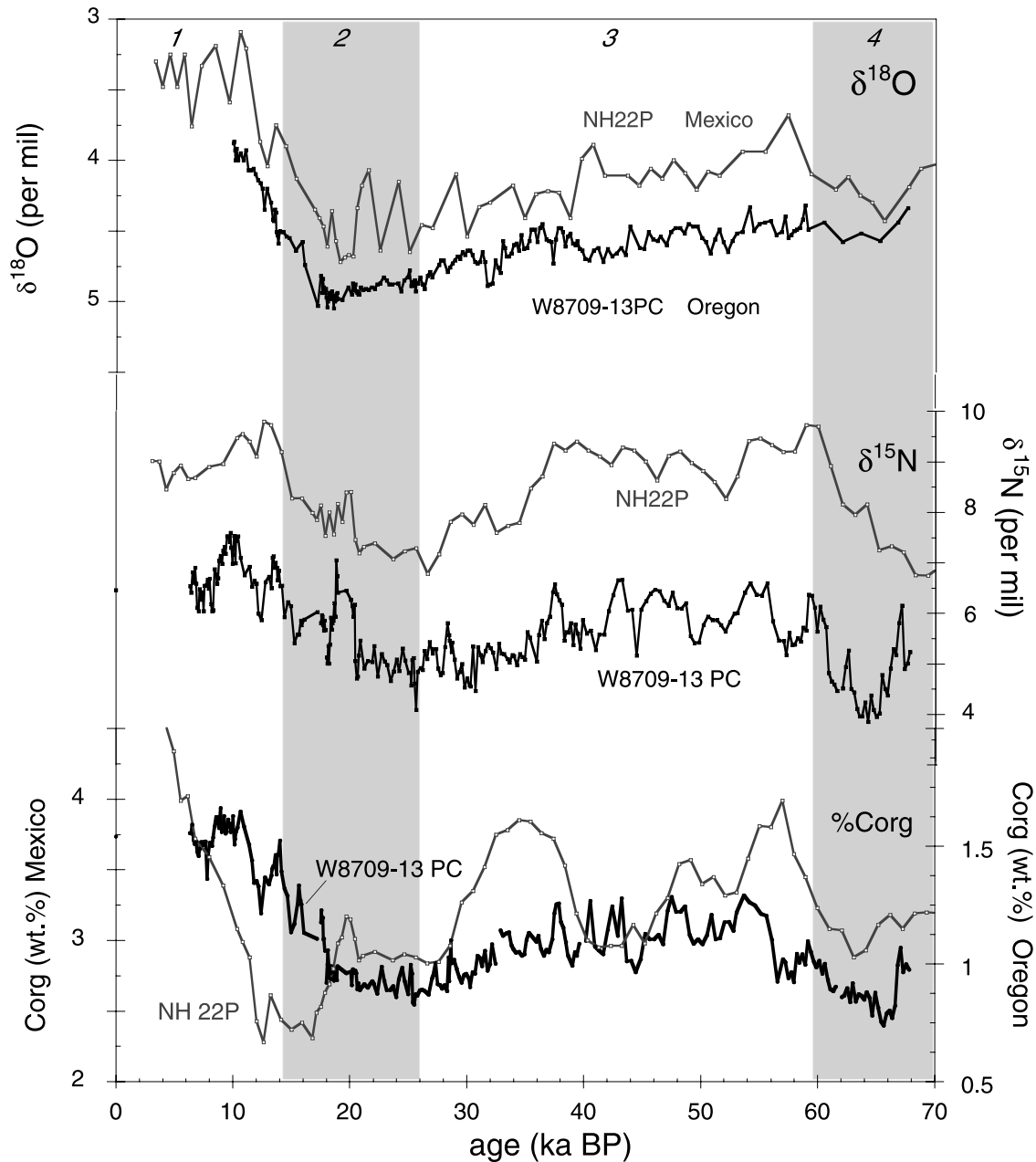


Figure 8. Comparison of benthic $\delta^{18}\text{O}$, $\delta^{15}\text{N}$, and percent C_{org} of Mexican margin core NH22P and Oregon core W8709-13PC plotted according to their independent chronologies. NH22P data and timescale are from *Ganeshram et al.* [2000] and *Ganeshram and Pedersen* [1998]. W8709-13PC $\delta^{18}\text{O}$ data are from *Lund and Mix* [1998], and chronology is from *Mix et al.* [1999] and *Lund and Mix* [1998]. Diamonds on y axes in middle and bottom graphs indicate surface sediment values at the Oregon site. Note that the y axis is different for both sites in the bottom graph. The glacial-interglacial $\delta^{18}\text{O}$ transition is recorded at the same time at both sites (± 500 years). Note the synchronous response in $\delta^{15}\text{N}$ but the lag in percent C_{org} off Mexico.

in turn indicates that the chronologies of both cores are accurate enough to allow an intercomparison between both records (within an error margin of ± 0.5 kyr). Comparing $\delta^{15}\text{N}$ in both cores shows that the glacial-interglacial $\delta^{15}\text{N}$ variations occur approximately synchronously at these two sites (Figure 8, middle), giving support to the vital role of the CUC in transporting isotopically heavy nitrate north-

ward. Comparing down core organic carbon concentration profiles, on the other hand, indicates that the glacial-interglacial $\% \text{C}_{\text{org}}$ transition in Mexico lags that off Oregon by several thousand years (Figure 8, bottom). Acknowledging that organic carbon burial might be affected by changes in sediment accumulation rate at each site, we also compare organic carbon concentrations normalized to alu-

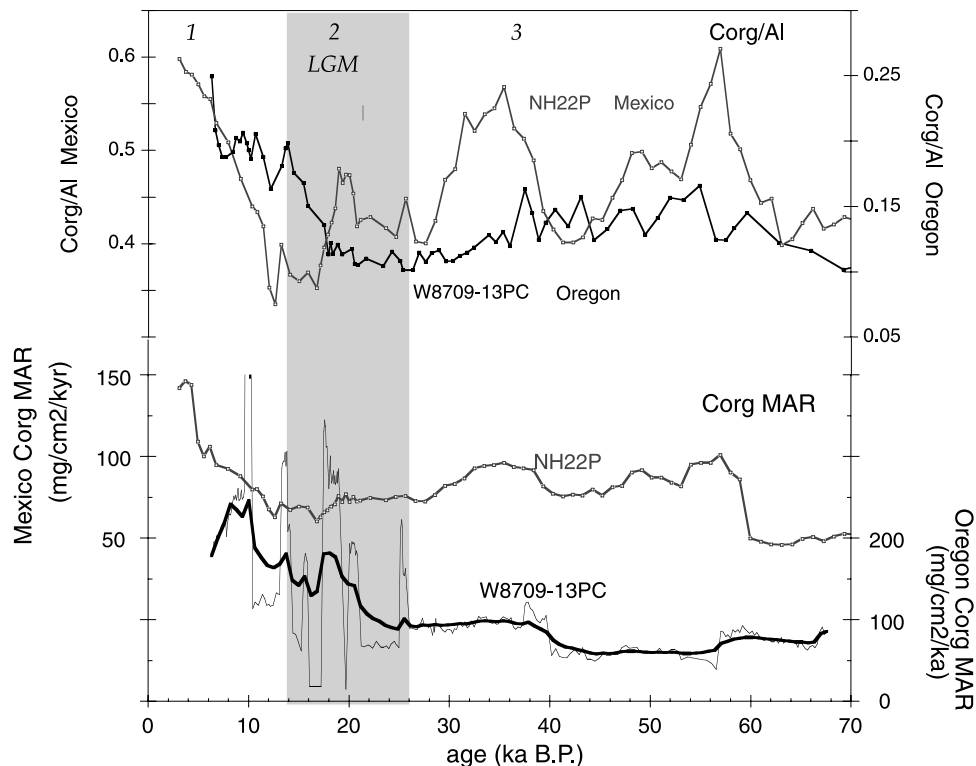


Figure 9. C_{org}/Al ratio and C_{org} accumulation rate records of Mexican margin core NH22P and Oregon core W8709-13PC plotted according to their independent chronologies. W8709-13PC C_{org}/Al data are from Dean *et al.* [1997] and Gardner *et al.* [1997]; see Figure 8 for other references. Thick solid line in the bottom graph is the smoothed average accumulation rate in Oregon core W8709-13PC. Note that y axes are different for each site.

minimum (C_{org}/Al) and C_{org} mass accumulation rates in both cores (Figure 9). Changes in C_{org}/Al ratios confirm the temporal offset between both sites. Comparing mass accumulation rates is more ambiguous. The close spacing of ^{14}C dates in Nearshore core W8709-13PC leads to abrupt changes in sedimentation rates, which directly translate into abrupt changes in C_{org} mass accumulation rates. Nevertheless, the general C_{org} accumulation rate increase after the last glacial seems to occur earlier off Oregon than off Mexico. Taken together, these records strongly suggest that the temporal offset between the two sites is a robust feature. It seems to indicate a so far undescribed time-transgressive development of upwelling-favorable northerly winds along the NW American coast after the last glacial, with those in the north ($\sim 40^\circ\text{N}$) increasing several kiloyears earlier than those in the south ($\sim 20^\circ\text{N}$).

[40] Relative to $\delta^{18}\text{O}$ benthic, $\%C_{\text{org}}$ increases approximately synchronously off Oregon (Figure 8) but lags $\delta^{18}\text{O}$ off Mexico [Ganeshram *et al.*, 2000, Figure 3]. Recently, Herbert *et al.* [2001] found that sea surface temperatures (SSTs) in the CC region warmed 10,000 to 15,000 years in advance of deglaciation as recorded by benthic $\delta^{18}\text{O}$. This earlier SST warming is most pronounced in the central CC (32°N) and somewhat smaller at the northern limb of the CC (41°N). It is thought to represent a collapse of the relatively cool CC during maximum glaciation, allowing the warmer gyre waters to move shoreward. South of the

modern CC (22°N), early deglacial warming is absent and SST rose in concert with deglaciation and benthic $\delta^{18}\text{O}$ [Herbert *et al.*, 2001]. Combining our findings with those of Herbert *et al.* [2001] south of the CC, it follows that primary production and upwelling-favorable winds lag SST and $\delta^{18}\text{O}$ benthic by several kiloyears after the LGM in this region. At the northern limb of the CC however, primary production rises synchronously with $\delta^{18}\text{O}$ and only slightly lags SST. As the Cordilleran and Laurentide ice sheets melted back (and $\delta^{18}\text{O}$ benthic rises), one would expect to see an increase in upwelling along the NW American margin [Kutzbach, 1987; COHMAP, 1988; Lyle *et al.*, 1992]. The Oregon records thus fit this picture but the apparent delay of upwelling to the south is not easily explained within the current understanding of climate evolution after the LGM. There does not seem to be a significant difference in mean insolation forcing between 40°N and 20°N [Laskar, 1990]. We speculate that the more northern latitudes might be more sensitive to atmospheric changes caused by the melting ice sheet. Alternatively, there might be yet unknown conditions in the tropical ocean that prevent northerly winds to develop in concert with the melting ice. Hindcasting these regionally diverse responses of single components in the ocean atmosphere system and examining their apparent decoupling using climate modeling will eventually lead to a better understanding of the climate system.

9. Summary and Implications

[41] Annual nitrate utilization off Oregon is complete and there is no significant diagenetic alteration of the $\delta^{15}\text{N}_{\text{PN}}$ signal in the water column or at the sediment-water interface. Combined with similar findings farther south, this observation makes sedimentary $\delta^{15}\text{N}$ a reliable tracer of subsurface nitrate along the NW American margin from at least 20° to 45°N . Isotopically heavy nitrate generated in the ETNP today is exported northward along the NW American coast via the CUC to at least 45°N . Although subsurface $\delta^{15}\text{N}_{\text{nitrate}}$ values decrease progressively toward the north, they are still higher than the global deep water average in the entire CCS region. Consequently, isotopically heavy nitrate is recorded at sites far beyond the boundaries of the denitrification zone in the ETNP.

[42] The glacial-interglacial pattern in sedimentary $\delta^{15}\text{N}$ is remarkably similar in timing and amplitude along the entire NW American margin, despite a general decrease in $\delta^{15}\text{N}$ values away from the ETNP. High values during the Holocene, oxygen isotope stage 5 and some periods during stage 3 at the Oregon sites most likely reflect relatively strong denitrification in the ETNP and a strong CUC. Approximately at the same time, paleoproduction indicators imply coastal upwelling was active off Oregon. During glacial stages 2 and 4, $\delta^{15}\text{N}$ values are relatively low and coastal upwelling strength off Oregon was significantly reduced. To a lesser degree, upwelling was also reduced between 13.6 and 11.6 ka B.P., a period possibly correlative with the Younger Dryas and during millennial-scale intervals in stage 3, which seem to occur on a similar frequency as Heinrich events in the North Atlantic. While sedimentary $\delta^{15}\text{N}$ and paleoproduction indicators vary approximately synchronously in records outside the modern denitrification zone, $\delta^{15}\text{N}$ clearly leads paleoproduction proxies within the ETNP after the LGM and at the stage 4/3 and 6/5 boundaries by several kiloyears. This lead implies a decoupling in the vertical dimension of surface and subsurface processes

during the glacial-interglacial and stadial/interstadial transitions.

[43] Circulation changes in the equatorial Pacific offer an explanation for this decoupling. Stronger easterlies during cold periods, such as the LGM, Heinrich events and Dansgaard-Oeschger stadials, would force a stronger EUC and increase oxygen advection into the ETNP, thereby reducing denitrification. During warm periods of low O_2 advection and strong denitrification, the CUC could transport heavy nitrate northward in a similar fashion as today. In contrast to local productivity change by itself, this mechanism can accommodate the decoupling of local surface production and denitrification rates in the ETNP. At the same time, it provides an atmospheric link between denitrification intensity in the eastern Pacific, horizontal advection of heavy nitrate into the midlatitude eastern Pacific and global climate change.

[44] Along the northwest American margin, northerly, coastal upwelling favorable winds seem to have intensified in a time-transgressive fashion after the LGM with those in the north ($\sim 40^\circ\text{N}$) starting several kiloyears before those in the south ($\sim 20^\circ\text{N}$). Together with recent results by *Herbert et al.* [2001], this points to a regionally diverse response of single components of the ocean-atmosphere system within the NE Pacific.

[45] **Acknowledgments.** We are very grateful to Robert Collier, Jack Dymond, Mitch Lyle and Alan Mix for sharing the Multitracers material, to Mark Altabet, Joe Needoba, and Markus Kienast for $\delta^{15}\text{N}_{\text{nitrate}}$ analyses, to Thomas Naehr for providing water samples and to Maureen Soon and Bente Nielsen for laboratory assistance. We thank Andy Bush and Markus Kienast for stimulating discussion, and Lex van Geen and Mark Altabet for official reviews that greatly helped to improve the manuscript. The Multitracers field work was supported by NSF grants OCE-8609366 and OCE-8919956. Core and sediment trap material was provided by the Core Repository of Oregon State University, supported by NSF grants OCE88-00458. This work was supported by NSERC through grants to S.E.C. and T.F.P. S.S.K. acknowledges support from the DAAD and the ICSS. The data will be available from the World Data center at <http://www.ngdc.noaa.gov/paleo/data.html>.

References

- Altabet, M. A., Variations in nitrogen isotopic composition between sinking and suspended particles: Implications for nitrogen cycling and particle transformation in the open ocean, *Deep Sea Res.*, 35(4), 535–554, 1988.
- Altabet, M. A., Nitrogen and carbon isotopic tracers of the source and transformation of particles in the deep sea, in *Particle Flux in the Ocean, 1996 SCOPE*, edited by P. J. Depetris, pp. 155–183, John Wiley, New York, 1996.
- Altabet, M. A., and R. François, Sedimentary nitrogen isotopic ratio as a recorder for surface ocean nitrate utilization, *Global Biogeochem. Cycles*, 8(1), 103–116, 1994.
- Altabet, M. A., R. François, D. W. Murray, and W. L. Prell, Climate-related variations in denitrification in the Arabian Sea from sediment $^{15}\text{N}/^{14}\text{N}$ ratios, *Nature*, 373, 506–509, 1995.
- Altabet, M. A., and J. J. McCarthy, Temporal and spatial variations in the natural abundance of ^{15}N in PON from a warm-core ring, *Deep Sea Res.*, 32(7), 755–772, 1985.
- Altabet, M. A., D. A. Murray, and W. L. Prell, Climate-linked oscillations in Arabian Sea denitrification over the last 1 Ma: Implications for the marine N-cycle, *Paleoceanography*, 14(6), 732–743, 1999a.
- Altabet, M. A., C. Pilskaln, R. Thunell, C. Pride, D. Sigman, F. Chavez, and R. Francois, The nitrogen isotope biogeochemistry of sinking particles from the margin of the eastern North Pacific, *Deep Sea Res.*, 146, 655–679, 1999b.
- Altabet, M. A., M. J. Higginson, and D. M. Murray, The effect of millennial-scale changes in Arabian Sea denitrification on atmospheric CO_2 , *Nature*, 415, 159–162, 2002.
- Andreasen, D. H., A. C. Ravelo, and A. J. Broccoli, Remote forcing at the Last Glacial Maximum in the tropical Pacific Ocean, *J. Geophys. Res.*, 106(C1), 879–897, 2001.
- Andreasen, D. J., and A. C. Ravelo, Tropical Pacific Ocean thermocline depth reconstruction for the Last Glacial Maximum, *Paleoceanography*, 12(3), 395–413, 1997.
- Archer, D. E., What controls opal preservation in tropical deep-sea sediments?, *Paleoceanography*, 8(1), 7–21, 1993.
- Bishop, J. K. B., The barite-opal-organic carbon association in oceanic particulate matter, *Nature*, 332, 341–343, 1988.
- Brandes, J. A. G., Isotopic effects of denitrification in the marine environment, Ph.D. thesis, Univ. of Wash., Seattle, 1996.
- Brandes, J. A., A. H. Devol, T. Yoshinari, D. A. Jayakumar, and S. W. A. Naqvi, Isotopic composition of nitrate in the central Arabian Sea and eastern tropical North Pacific: A tracer for mixing and nitrogen cycles, *Limnol. Oceanogr.*, 43(7), 1680–1689, 1998.
- Bush, A. B. G., and S. G. H. Philander, The climate of the Last Glacial Maximum: Results from a coupled atmosphere-ocean general circulation model, *J. Geophys. Res.*, 104(D20), 24,509–24,525, 1999.
- Calvert, S. E., and N. B. Price, Geochemistry of Namibian Shelf sediments, in *Coastal Upwelling*, edited by J. Thiede, pp. 337–375, Plenum, New York, 1983.
- Calvert, S. E., B. L. Cousens, and M. Y. S. Soon, An X-ray fluorescence spectrometric method for the determination of major and minor elements in ferromanganese nodules, *Chem. Geol.*, 51, 9–18, 1985.
- Calvert, S. E., R. M. Bustin, and T. F. Pedersen, Lack of evidence for enhanced preservation of

- sedimentary organic matter in the oxygen minimum of the Gulf of California, *Geology*, 20, 757–760, 1992.
- Calvert, S. E., T. F. Pederson, P. H. Naidu, and U. von Stackelberg, On the organic carbon maximum on the continental slope of the eastern Arabian Sea, *J. Mar. Res.*, 53, 269–296, 1995.
- Castro, C. G., F. P. Chavez, and C. A. Collins, Role of the California Undercurrent in the export of denitrified waters from the eastern tropical North Pacific, *Global Biogeochem. Cycles*, 15(4), 819–830, 2001.
- Chavez, F. P., R. T. Barber, M. Korso, A. Huyer, S. R. Ramp, T. P. Stanton, and B. R. D. Mendiola, Horizontal transport and the distribution of nutrients in the coastal transition zone off northern California: Effects on primary production, phytoplankton biomass and species composition, *J. Geophys. Res.*, 96(C8), 14,833–14,848, 1991.
- Church, T. M., and K. Wolgemuth, Marine barite saturation, *Earth Planet. Sci. Lett.*, 15, 35–44, 1972.
- Cline, J. D., and I. R. Kaplan, Isotopic fractionation of dissolved nitrate during denitrification in the eastern tropical North Pacific Ocean, *Mar. Chem.*, 3, 271–299, 1975.
- Codispoti, L. A., Phosphorus vs nitrogen limitation of new and export production, in *Productivity of the Ocean: Present and Past*, edited by G. Wefer, pp. 377–394, John Wiley, New York, 1989.
- Codispoti, L. A., and J. P. Christensen, Nitrification, denitrification and nitrous oxide cycling in the eastern tropical South Pacific Ocean, *Mar. Chem.*, 16, 277–300, 1985.
- COHMAP, Climatic changes of the last 18,000 years: Observations and model simulations, *Science*, 241, 1043–1052, 1988.
- Dean, W. E., J. V. Gardner, and D. Z. Piper, Inorganic geochemical indicators of glacial-interglacial changes in productivity and anoxia on the California continental margin, *Geochim. Cosmochim. Acta*, 61(21), 4507–4518, 1997.
- Doose, H., F. G. Prahl, and M. L. Lyle, Biomarker temperature estimates for modern and last glacial surface waters of the California Current System between 33° and 42°, *Paleoceanography*, 12(4), 615–622, 1997.
- Dugdale, R. C., and J. J. Goering, Uptake of new and regenerated forms of nitrogen in primary productivity, *Limnol. Oceanogr.*, 12, 196–206, 1967.
- Dymond, J., and R. Collier, Particulate barium fluxes and their relationships to biological productivity, *Deep Sea Res., Part II*, 43(4–6), 1283–1308, 1996.
- Dymond, J., and M. Lyle, Particle fluxes in the ocean and implications for sources and preservation of ocean sediments, in *Material Fluxes on the Surface of the Earth*, edited by W. Hay, pp. 125–142, Natl. Acad. Press, Washington, D. C., 1994.
- Dymond, J., E. Suess, and M. Lyle, Barium in deep-sea sediments: A geochemical proxy for paleoproductivity, *Paleoceanography*, 7(2), 163–181, 1992.
- Emmer, E., and R. C. Thunell, Nitrogen isotope variations in Santa Barbara Basin sediments: Implications for denitrification in the eastern tropical North Pacific during the last 50,000 years, *Paleoceanography*, 15(4), 377–387, 2000.
- Falkowski, P. G., Evolution of the nitrogen cycle and its influence on the biological sequestration of CO₂ in the ocean, *Nature*, 387, 272–275, 1997.
- Flohn, H., Oceanic upwelling as a key for abrupt climatic change, *J. Meteorol. Soc. Jpn.*, 60(1), 268–273, 1982.
- Franois, R., S. Honjo, S. J. Manganini, and G. E. Ravizza, Biogenic barium fluxes to the deep sea: Implications for paleoproductivity reconstruction, *Global Biogeochem. Cycles*, 9(2), 289–303, 1995.
- Ganeshram, R. S., and T. F. Pedersen, Glacial-interglacial variability in upwelling and bioproductivity off NW Mexico: Implications for Quaternary paleoclimate, *Paleoceanography*, 13(6), 634–645, 1998.
- Ganeshram, R. S., T. F. Pedersen, S. E. Calvert, and J. W. Murray, Large changes in oceanic nutrient inventories from glacial to interglacial periods, *Nature*, 376, 755–758, 1995.
- Ganeshram, R. S., T. F. Pedersen, S. E. Calvert, G. W. McNeill, and M. R. Fontugne, Glacial-interglacial variability in denitrification in the world's oceans: Causes and consequences, *Paleoceanography*, 15(4), 361–376, 2000.
- Gardner, G. A., Biological and hydrological evidence for Pacific equatorial water on the continental shelf of north of Vancouver Island British Columbia, *Can. J. Fish. Aquat. Sci.*, 39, 660–667, 1982.
- Gardner, J. V., W. Dean, and P. Dartnell, Biogenic sedimentation beneath the California Current system for the past 30 kyr and its paleoceanographic significance, *Paleoceanography*, 12(2), 207–225, 1997.
- Garfield, P. C., T. T. Packard, G. E. Friederich, and L. A. Codispoti, A subsurface particle maximum layer and enhanced microbial activity in the secondary nitrite maximum of the northeastern tropical Pacific Ocean, *J. Mar. Res.*, 41, 747–768, 1983.
- Hartnett, H. E., R. G. Keil, J. I. Hedges, and A. H. Devol, Influence of oxygen exposure time on organic carbon preservation in continental margin sediments, *Nature*, 391, 572–574, 1998.
- Hedges, J. I., J. A. Baldock, Y. Gilnas, C. Lee, M. Peterson, and S. G. Wakeham, Evidence for non-selective preservation of organic matter in sinking particles, *Nature*, 409, 801–804, 2001.
- Herbert, T. D., J. D. Schuffert, D. Andreasen, L. Heusser, M. Lyle, A. Mix, A. C. Ravelo, L. D. Stott, and J. C. Herguera, Collapse of the California Current during glacial maxima linked to climate change on land, *Nature*, 293, 71–76, 2001.
- Hickey, B. M., The California Current System—Hypotheses and facts, *Prog. Oceanogr.*, 8, 191–279, 1979.
- Hickey, B. M., Coastal oceanography of western North America from the tip of Baja California to Vancouver Island, in *The Sea*, edited by K. H. Brink, pp. 345–391, John Wiley, New York, 1998.
- Hood, R. R., M. R. Abbott, A. Huyer, and P. M. Korso, Surface patterns in temperature, flow, phytoplankton biomass, and species composition in the coastal zone off northern California, *J. Geophys. Res.*, 95(C10), 18,081–18,094, 1990.
- Hood, R. R., M. R. Abbott, and A. Huyer, Phytoplankton and photosynthetic light response in the coastal transition zone off northern California in June 1987, *J. Geophys. Res.*, 96(C8), 14,769–14,780, 1991.
- Hostetler, S. W., and P. J. Bartlein, Simulation of the potential responses of regional climate and surface processes in western North America to a canonical Heinrich event, in *Mechanisms of Global Climate Change at Millennial Time Scales*, *Geophys. Monogr. Ser.*, vol. 112, edited by P. U. Clark, R. S. Webb and L. D. Keigwin, pp. 313–328, AGU, Washington, D. C., 1999.
- Huyer, A., Coastal upwelling in the California current system, *Prog. Oceanogr.*, 12, 259–284, 1983.
- Huyer, A., and R. L. Smith, The signature of El Niño off Oregon, *J. Geophys. Res.*, 90(C4), 7133–7142, 1985.
- Karlin, R., M. Lyle, and R. Zahn, Carbonate variations in the NE-Pacific during the late Quaternary, *Paleoceanography*, 7, 43–61, 1992.
- Kienast, M., Unchanged nitrogen isotope composition of organic matter in the South China Sea during the last climatic cycle: Global implications, *Paleoceanography*, 15, 244–253, 2000.
- Kutzbach, J. E., Model simulations of the climatic patterns during the deglaciation of North America, in *North America and Adjacent Oceans During the Last Deglaciation*, edited by H. E. J. Wright, pp. 425–446, Geol. Soc. of Am., Boulder, Colo., 1987.
- Laskar, J., The chaotic motion of the solar system: A numerical estimate of the chaotic zones, *Icarus*, 88, 266–291, 1990.
- Law, C. S., and N. J. P. Owens, Significant flux of atmospheric nitrous oxide from the northwestern Indian Ocean, *Nature*, 346, 826–828, 1990.
- Levitus, S., T. Boyer, R. Burgett, and M. Conkright, *World Ocean Atlas*, Natl. Oceanogr. Data Cent., Natl. Oceanic and Atmos. Admin, Silver Spring, Md., 1994.
- Liu, K.-K., and I. R. Kaplan, The eastern tropical Pacific as a source of ¹⁵N-enriched nitrate in seawater off southern California, *Limnol. Oceanogr.*, 34(5), 820–830, 1989.
- Lukas, R., The termination of the Equatorial Undercurrent in the eastern Pacific, *Prog. Oceanogr.*, 16, 63–90, 1986.
- Lund, D. C., and A. C. Mix, Millennial-scale deep water oscillations: Reflections of the North Atlantic in the deep Pacific from 10 to 60 ka, *Paleoceanography*, 13, 10–19, 1998.
- Lyle, M., R. Zahn, F. Prahl, J. Dymond, R. Collier, N. Pisias, and E. Suess, Paleoproductivity and carbon burial across the California Current: The Multitracers transect, 42°N, *Paleoceanography*, 7, 251–272, 1992.
- Lyle, M., A. Mix, C. Ravelo, D. Andreasen, L. Heusser, and A. Olivarez, Millennial-scale CaCO₃ and C_{org} events along the northern and central California Margin: Stratigraphy and origins, *Proc. Ocean Drill. Program Sci. Results*, 167, 163–182, 2000.
- Lyle, M., L. Heusser, T. Herbert, A. Mix, and J. Barron, Interglacial theme and variations: 500 k.y. of orbital forcing and associated responses from the terrestrial and marine biosphere U.S. Pacific Northwest, *Geology*, 29(12), 1115–1118, 2001.
- McElroy, M. B., Marine biological controls on atmospheric CO₂ and climate, *Nature*, 302, 328–329, 1983.
- Mix, A. C., D. C. Lund, N. G. Pisias, P. Bodn, L. Bornmalm, M. Lyle, and J. Pike, Rapid climate oscillation in the northeast Pacific during the last deglaciation reflects Northern and Southern Hemisphere sources, in *Mechanisms of Global Climate Change at Millennial Time Scales*, *Geophys. Monogr. Ser.*, vol. 112, edited by P. U. Clark, R. S. Webb and L. D. Keigwin, pp. 127–148, AGU, Washington, D. C., 1999.
- Molina-Cruz, A., The relation of the southern trade-winds to upwelling processes during the last 75 000 years, *Quat. Res.*, 8, 324–338, 1977.
- Mortlock, R. A., and P. N. Froelich, A simple method for the rapid determination of biogenic opal in pelagic marine sediments, *Deep Sea Res.*, 36, 1415–1426, 1989.

- Müller, P. J. S. E., Productivity, sedimentation rate, and sedimentary organic matter in the oceans I, Organic carbon preservation, *Deep Sea Res.*, 26, 1347–1362, 1979.
- Naqvi, S. W. A., T. Yoshinari, D. A. Jayakumar, M. A. Altabet, P. V. Narvekar, A. H. Devol, J. A. Brandes, and L. A. Codispoti, Budgetary and biogeochemical implications of N_2O isotopes signatures in the Arabian Sea, *Nature*, 394, 462–466, 1998.
- Naqvi, S. W. A., D. A. Jayakumar, P. V. Narvekar, H. Naik, V. V. S. S. Sarma, W. D'Souza, S. Joseph, and M. D. George, Increased marine production of N_2O due to intensifying anoxia on the Indian continental shelf, *Nature*, 408, 346–349, 2000.
- Nelson, D. M., P. Treguer, M. A. Brzezinski, A. Leynaert, and B. Queguiner, Production and dissolution of biogenic silica in the ocean: Revised global estimates, comparison with regional data and relationship to biogenic sedimentation, *Global Biogeochem. Cycles*, 9(3), 359–372, 1995.
- Nicholson, S. E., and H. Flohn, African environmental and climatic changes and the general atmospheric circulation in late Pleistocene and Holocene, *Clim. Change*, 2, 313–348, 1980.
- Ortiz, J., A. Mix, S. Hostetler, and M. Kashgarian, The California Current of the Last Glacial Maximum: Reconstruction at 42°N based on multiple proxies, *Paleoceanography*, 12, 191–205, 1997.
- Parkin, D. W., and N. J. Shackleton, Trade wind and temperature correlations down a deep-sea core off the Sahara Coast, *Nature*, 245, 455–457, 1973.
- Paytan, A., M. Kastner, and F. P. Chavez, Glacial to interglacial fluctuations in productivity in the Equatorial Pacific as indicated by marine barite, *Science*, 274, 1355–1357, 1996.
- Pedersen, T. F., Increased productivity in the eastern equatorial Pacific during the Last Glacial Maximum (19 000 to 14 000 yr B P.), *Geology*, 11(1), 16–19, 1983.
- Pedersen, T. F., G. B. Shimmiel, and N. B. Price, Lack of enhanced preservation of organic matter in sediments under the oxygen minimum on the Oman Margin, *Geochim. Cosmochim. Acta*, 56, 545–551, 1992.
- Philander, S. G. H., *El Niño, La Niña, and the Southern Oscillation*, 293 pp., Academic, San Diego, Calif., 1990.
- Pierce, S. D., R. L. Smith, P. M. Kosro, J. A. Barth, and C.D. Wilson, Continuity of the poleward undercurrent along the eastern boundary of the mid-latitude north Pacific, *Deep Sea Res., Part II*, 47, 738–810, 2000.
- Pisias, N. G., A. C. Mix, and L. Heusser, Millennial scale climate variability of the northeast Pacific Ocean and northwest North America based on radiolaria and pollen, *Quat. Sci. Rev.*, 20, 1561–1576, 2001.
- Pride, C., R. Thunell, D. Sigman, L. Keigwin, and M. Altabet, Nitrogen isotopic variations in the Gulf of California since the last deglaciation: Response to global climate change, *Paleoceanography*, 14, 397–409, 1999.
- Ragueneau, O., et al., A review of the Si cycle in the modern ocean: Recent progress and missing gaps in the application of biogenic opal as a paleoproductivity proxy, *Earth Planet. Sci. Lett.*, 26, 317–365, 2000.
- Sancetta, C., Comparison of phytoplankton in sediment trap time series and surface sediments along a productivity gradient, *Paleoceanography*, 7, 183–194, 1992.
- Sancetta, C., M. Lyle, L. Heusser, and R. Zahn, Late glacial to Holocene changes in upwelling regimes and seasonal production of the northern California Current system, *Quat. Res.*, 1992.
- Sarnthein, M. W. K., Global variations of surface ocean productivity in low and mid latitudes: Influence on CO_2 reservoirs of the deep ocean and atmosphere during the last 21,000 years, *Paleoceanography*, 3, 361–399, 1988.
- Sarnthein, M., G. Tetzlaff, B. Koopmann, K. Wolter, and U. Pflaumann, Glacial and interglacial wind regimes over the eastern subtropical Atlantic and north-west Africa, *Nature*, 293, 193–196, 1981.
- Sigman, D., M. Altabet, R. Michener, D. McCorkle, B. Fry, and R. M. Holmes, Natural abundance-level measurement of the nitrogen isotopic composition of oceanic nitrate: An adaptation of the ammonia diffusion method, *Mar. Chem.*, 57, 227–242, 1997.
- Stott, L. D., W. Berelson, R. Douglas, and D. Gorsline, Increased dissolved oxygen in Pacific intermediate waters due to lower rates of carbon oxidation in sediments, *Nature*, 407, 367–370, 2000.
- Suess, E., Particle organic carbon flux in the oceans-surface productivity and oxygen utilization, *Nature*, 288, 1980.
- Thunell, R. C., R. Varela, M. Llano, J. Collister, F. Muller-Karger, and R. Bohrer, Organic carbon fluxes, degradation and accumulation in an anoxic basin: Sediment trap results from the Cariaco Basin, *Limnol. Oceanogr.*, 45, 300–308, 2000.
- Toggweiler, J., K. Dixon, and W. Broecker, The Peru upwelling and the ventilation of the South Pacific thermocline, *J. Geophys. Res.*, 96(C11), 20,467–20,497, 1991.
- Tsuchiya, M., The origin of the Pacific equatorial ^{13}C water, *J. Phys. Oceanogr.*, 11, 794–812, 1981.
- Tsuchiya, M., R. Lukas, R. A. Fine, E. Firing, and E. Lindstrom, Source waters of the Pacific Equatorial Undercurrent, *Prog. Oceanogr.*, 23, 101–147, 1989.
- Van Geen, A., R. K. Takesue, J. Goddard, T. Takahashi, J. A. Barth, and R. L. Smith, Carbon and nutrient dynamics during coastal upwelling off Cape Blanco, Oregon, *Deep Sea Res., Part II*, 47, 975–1002, 2000.
- Verardo, D. J., P. N. Froelich, and A. McIntyre, Determination of organic carbon and nitrogen in marine sediments using the Carlo Erba NA-1500 Analyzer, *Deep Sea Res.*, 37, 157–165, 1990.
- Voss, M., J. W. Dippner, and J. P. Montoya, Nitrogen isotope patterns in the oxygen-deficient waters of the eastern tropical North Pacific Ocean, *Deep Sea Res., Part I*, 1905–1921, 2001.
- Wada, E., and A. Hattori, Natural abundance of ^{15}N in particulate organic matter in the North Pacific Ocean, *Geochim. Cosmochim. Acta*, 40, 249–251, 1976.
- Wada, E., and A. Hattori, Nitrogen isotope effects in the assimilation of inorganic nitrogenous compounds by marine diatoms, *Geomicrobiol. J.*, 1(1), 85–101, 1978.
- Wooster, W. S., and J. H. Jones, California Undercurrent off northern Baja California, *J. Mar. Res.*, 28(2), 235–250, 1970.
- Wu, J.-P., S. E. Calvert, and C. S. Wong, Nitrogen isotope variations in the subarctic north-east Pacific: Relationships to nitrate utilization and trophic structure, *Deep Sea Res., Part I*, 44, 287–314, 1997.
- Wyrki, K., The oxygen minima in relation to ocean circulation, *Deep Sea Res.*, 9, 11–23, 1962.
- Wyrki, K., Circulation and water masses in the eastern equatorial Pacific Ocean, *Int. J. Oceanol. Limnol.*, 1, 117–147, 1967.

S. E. Calvert, S. S. Kienast, and T. F. Pedersen, Earth and Ocean Sciences, University of British Columbia, 6270 University Boulevard, Vancouver, British Columbia, Canada V6T 1Z4. (skienast@eos.ubc.ca)